

ER-2808

SHIP SHOAL AREA BLOCK 229
RESERVOIR ENGINEERING STUDY

ARTHUR LAKES LIBRARY
COLORADO SCHOOL of MINES
GOLDEN, COLORADO 80401

by

Fernando Albuja R.

ProQuest Number: 10781146

All rights reserved

INFORMATION TO ALL USERS

The quality of this reproduction is dependent upon the quality of the copy submitted.

In the unlikely event that the author did not send a complete manuscript and there are missing pages, these will be noted. Also, if material had to be removed, a note will indicate the deletion.



ProQuest 10781146

Published by ProQuest LLC (2018). Copyright of the Dissertation is held by the Author.

All rights reserved.

This work is protected against unauthorized copying under Title 17, United States Code
Microform Edition © ProQuest LLC.

ProQuest LLC.
789 East Eisenhower Parkway
P.O. Box 1346
Ann Arbor, MI 48106 – 1346

A thesis submitted to the Faculty and the Board of Trustees of Colorado School of Mines in partial fulfillment of the requirements for the degree of Master of Engineering (Petroleum Engineer).

Golden, Colorado

Date Sept. 20, 1983

Signed: *Fernando Albuja R.*
Fernando Albuja R.

Approved: *Dan M. Bass*
Dr. Daniel M. Bass
Thesis Advisor

Golden, Colorado

Date Sept. 21, 1983

Craig W. Van Kirk
Craig W. Van Kirk :k
:m
:nt
Dr. Craig W. Van Kirk

ABSTRACT

A reservoir study of the Ship Shoal Area Block 229 Field located offshore Louisiana is presented. The primary objective of the study was the estimation of oil reserves, and the prediction of future performance of the centrally located TP13-A Sand oil reservoir.

The original oil-in-place calculated by volumetrics and by material balance was estimated to be 10.3 million STB. There was an excellent agreement between the two methods of determining oil-in-place.

The oil recovery to date has been about 33 percent of the stock-tank oil originally in-place, and it is estimated that an ultimate recovery of 47 percent is attainable.

The drive mechanism is primarily solution-gas with gravity segregation, although a finite aquifer contributes to some pressure support.

TABLE OF CONTENTS

	Page
ABSTRACT	iii
LIST OF FIGURES	vi
LIST OF TABLES	viii
ACKNOWLEDGMENTS	ix
INTRODUCTION	1
REGIONAL AND FIELD GEOLOGY	5
DEVELOPMENT AND PRODUCTION HISTORY	9
RESERVOIR PARAMETERS	23
RESERVOIR ROCK PROPERTIES	23
Porosity	23
Permeability	27
Connate Water Saturation	28
Effective Pay thickness	32
RESERVOIR FLUID PROPERTIES	32
VOLUMETRIC DETERMINATION OF ORIGINAL OIL-IN-PLACE	43
MATERIAL BALANCE PAST PERFORMANCE CALCULATIONS	51
FUTURE PERFORMANCE CALCULATIONS	61
CONCLUSIONS	75
REFERENCES CITED	77
NOMENCLATURE	79
APPENDICES	
A: DERIVATION OF THE MATERIAL BALANCE EQUATION AS AN EQUATION OF A STRAIGHT LINE.	80
B: PROGRAM TO CALCULATE THE X, Y VALUES FROM THE	

MATERIAL BALANCE EQUATION AS AN EQUATION OF A
STRAIGHT LINE, FOR A SATURATED OIL RESERVOIR. 84

C: PROGRAM TO PREDICT THE FUTURE BEHAVIOR OF A
SATURATED OIL RESERVOIR, USING THE MATERIAL
BALANCE AS AN EQUATION OF A STRAIGHT LINE 86

LIST OF FIGURES

Figure	Page
1. Location Map Of The Ship Shoal Area Block 229.....	2
2. TP13-A Sand Productive Limits.....	3
3. TP13-A Sand Typical Electric Log, Well A-1.....	6
4. TP13-A Sand Net Pay Isopachous Maps.....	8
5. Well A-1 Production History.....	10
6. Well A-2 Production History.....	11
7. Well A-3 Production History.....	12
8. Well A-4 Production History.....	13
9. Well A-7 Production History.....	14
10. Well A-9 Production History.....	15
11. Well A-11 Production History.....	16
12. Well A-16 Production History.....	17
13. Well A-17 Production History.....	18
14. Well A-19 Production History.....	19
15. Well A-20 Production History.....	20
16. Field Production Curves.....	21
17. Porosity Histogram For Samples Of TP13-A Sand.....	26
18. Neutron-Density Frequency Cross-Plot.....	30
19. Solution Gas-Oil Ratio vs Pressure.....	34
20. Oil Formation Volume Factor vs Pressure.....	38
21. Oil Viscosity vs Pressure.....	39
22. Gas Deviation Factor vs Pressure.....	40

23. Gas Formation Volume Factor vs Pressure.....	41
24. Gas Viscosity vs Pressure.....	42
25. Top Of TP13-A Sand Structure Map.....	44
26. Bottom Of TP13-A Sand Structure Map.....	45
27. Structural Distribution Net Productive Sand.....	46
28. Average Reservoir Pressure vs Cumulative Oil Production.....	54
29. Average Reservoir Pressure vs Time.....	55
30. Calculation Of Original Oil-In-Place TP13-A Sand.....	58
31. Calculation Of Original Oil-In-Place TP13-A Sand For Different Values Of m.....	59
32. Gas-Oil Relative Permeability Ratio vs Oil Saturation.....	63
33. Pore-Volume Distribution and Well Completion Location in The Pore Volume.....	66
34. Decline Curve For TP13-A Sand.....	67
35. Predicted Pressure vs Cumulative Oil Production.....	69
36. Predicted Pressure vs Time.....	71
37. Predicted Producing Gas-Oil Ratio vs Cumulative Oil Production.....	73
38. Predicted Cumulative Water Influx vs Cumulative Production.....	74

LIST OF TABLES

Table	Page
1. Summary Of The Average Reservoir Properties.....	24
2. Classification of Porosity Data.....	25
3. Calculation Of Geometric Mean Permeability.....	29
4. Example Log Calculations.....	33
5. Calculation Of Net Oil Sand Volume From Isopachous Map.....	47
6. Calculation Of Net Gas Sand Volume From Isopachous Map.....	48
7. Input Data For Material Balance Calculations.....	52
8. Bottom-Hole Pressure Data.....	53
9. Results Of Decline Curve Analysis.....	68
10. Summary Of Future Predictions Calculations.....	70

ACKNOWLEDGMENT

I wish to express gratitude to Dr. Daniel M. Bass for acting as my thesis advisor, and for his valuable guidance during the preparation of this study.

The author thanks the Kerr-McGee Corporation for kindly supplying the basic data used in this study.

I am particularly indebted to my wife Maria Fernanda, and my daughters, M. Belen, M. Fernanda, and M. Jose, for their patient^{ce} and encouragement during my stay in the United States.

The author also wishes to express his gratitude to the Ecuadorian State Oil Corporation, "C.E.P.E.", and to the Fulbright Commission of Ecuador for giving him the opportunity to obtain a Master's Degree in Petroleum Engineering.

INTRODUCTION

The Ship Shoal Area Block 229 field is located offshore Terrebonne Parish, approximately 85 miles south-southeast of Morgan City, Louisiana at a water depth of approximately 130 feet. Figure 1 shows the location of the field.

The field produces from Miocene unconsolidated sand developments on the west flank of a piercement-type salt dome. The A Sand reservoir discussed in this report is not continuous throughout the area. A combination of normal faulting together with local shaling-out has divided the area into three essentially closed reservoirs.

The major hydrocarbon accumulation is located in the middle of the structure and will hereafter be referred to as TP13-A Sand reservoir (Figure 2, Region 2). Productive limits of the field are shown in Figure 2 which is contoured on the top of TP13-A Sand.

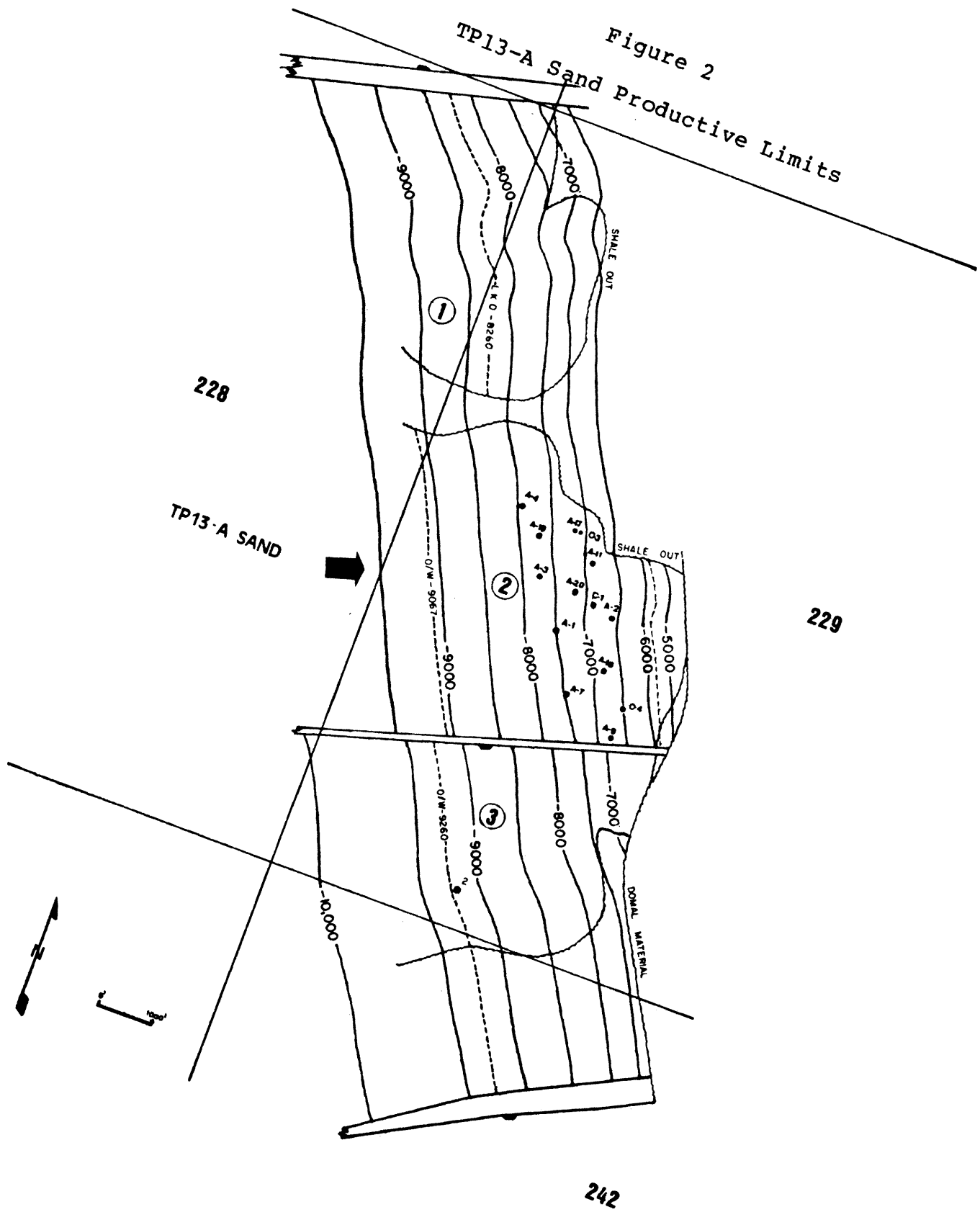
The TP13-A Sand oil reservoir was discovered in March, 1969, with the completion of the A-1 well by Kerr-McGee Corporation. Development proceeded rapidly on approximately 20 acre spacing. Since discovery, 14 oil productive wells have been drilled.

The field is a saturated black oil reservoir with an initial gas-cap and aquifer. The reservoir oil rate reached

Figure 1
Location Map Of The Ship Shoal Area Block 229



Figure 2
TP13-A Sand Productive Limits



its maximum in 1971 at 2,500 BOPD, with the completion of field development.

The primary purpose of this study is the estimation of original oil-in-place and the prediction of future performance of TP13-A Sand oil reservoir. Required data was obtained from conventional core analysis, well logs for each well (spontaneous-potential and induction), and production history from April, 1970, to November, 1982. Bottom-hole shut-in pressure data were also available, which permitted calculations using the material balance equation (MBE).

REGIONAL AND FIELD GEOLOGY

Three parallel radial faults striking SW-NE (Figure 2) control the vertical and horizontal extent of the flank reservoirs in the Ship Shoal Area Block 229 field. In most traps of this nature, faulting has influenced the amount of entrapped hydrocarbons (Halbouty, 1979).

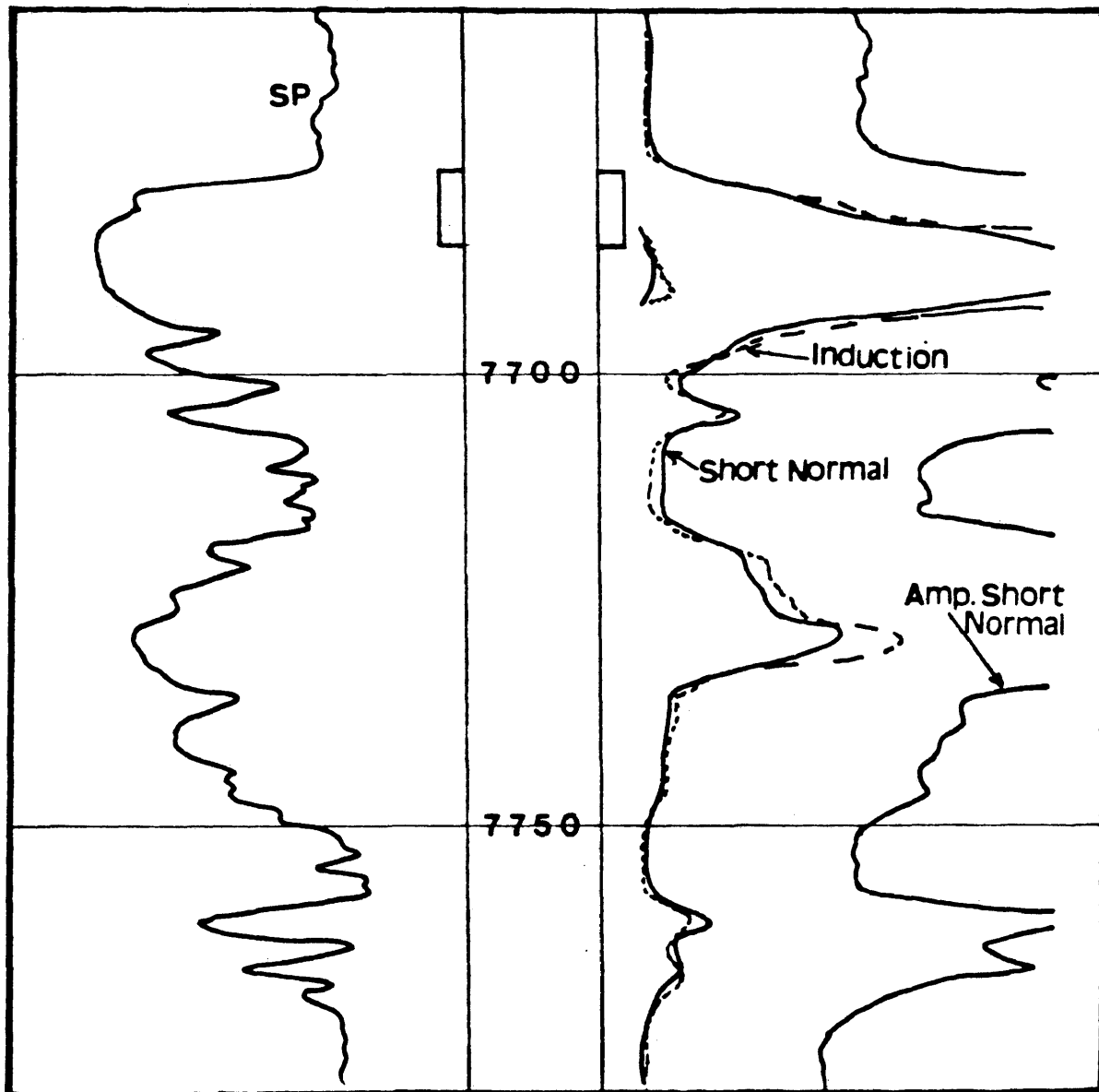
The centrally located TP13-A Sand of Miocene age dips at about 40 degrees away from the center of the salt intrusion, and like most traps on the flanks of piercement dome it shales out before reaching the salt core (Halbouty, 1979).

This productive sand is encountered at an average depth of 7,500 feet below mean sea level. It is closed on the south by a normal fault, on the north and on the east by sand shale out, and on the west by a water oil contact at 9,067 feet subsea. The dip of the fault is about 10 degrees SE, and the strike is SW-NE. The hydrocarbon trap is formed on the upthrown side of the fault.

Figure 3 is a typical electric log of this reservoir which can be described as a very fine to fine-grained, gray, soft sand with shale stringers. Core analysis of this zone indicates good oil show with erratic values of permeability.

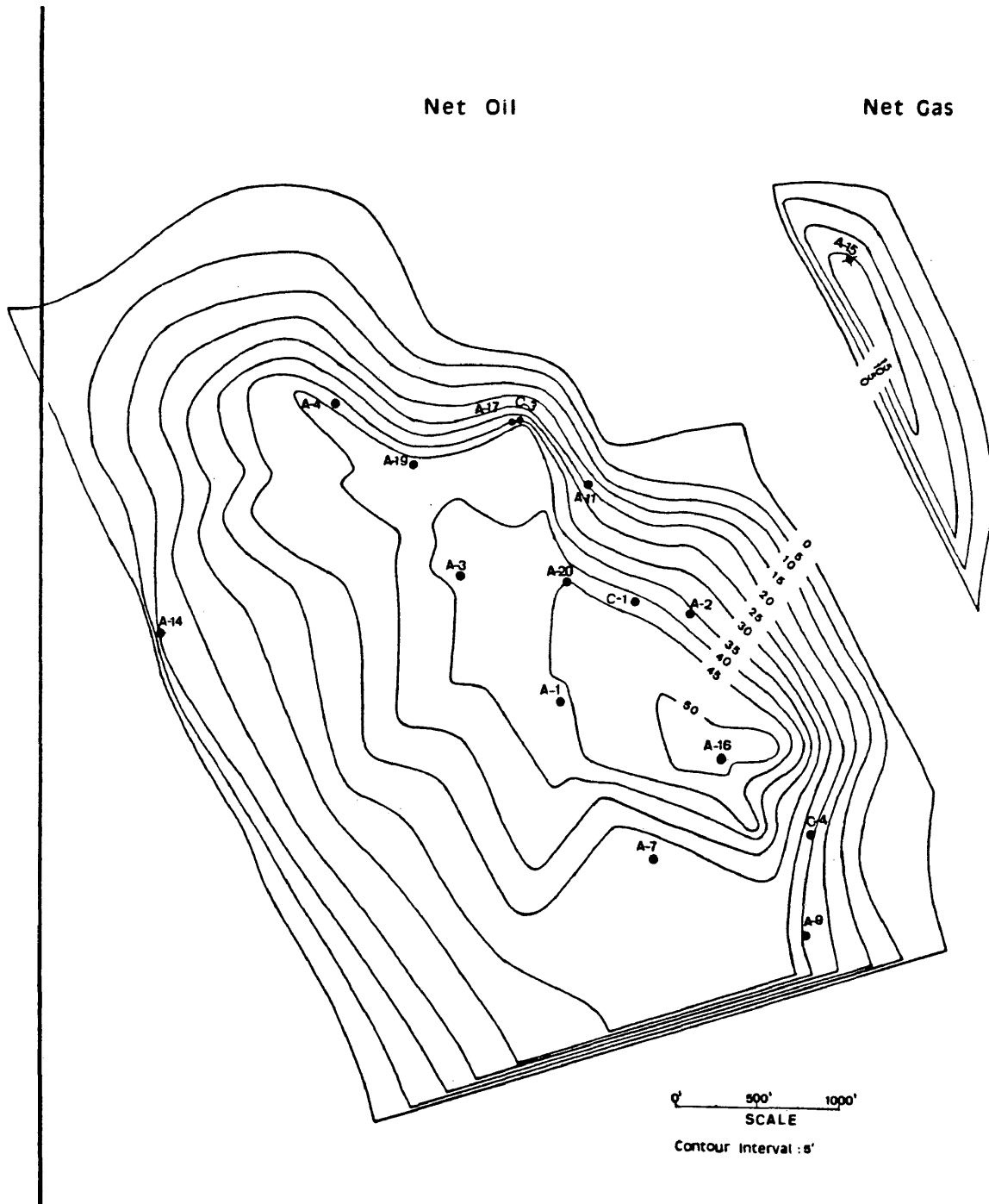
An examination of the TP13-A Sand oil-effective isopach

Figure 3
TP13-A Sand Typical Electric Log, Well A-1



map presented in Figure 4, shows that the sand thickness in the middle of the field is fairly uniform; however, laterally to the north and east the sand shales out rapidly.

Figure 4
TP13-A Sand Net Pay Isopachous Map



DEVELOPMENT AND PRODUCTION HISTORY

The TP13-A Sand oil reservoir was discovered with the completion of well A-1 in March, 1969, at an average depth of 7,587 feet subsea for an initial potential of 432 BOPD of 37.9 API gravity.

Development drilling began in May, 1970, and proceeded until July, 1971. Wells were directionally drilled from two platforms. Since most salt-dome reservoirs have active water drives, development wells were located at the highest structural position. A total of 20 wells, including 3 infill wells in 1982, were drilled. Of those, 14 were oil productive (4 presently shut-in). The field was placed on production during April, 1970. Initial production rates of the wells varied from a minimum of 180 BOPD to a maximum of 432 BOPD. Figures 5 to 15 show the individual production of the wells since their completion date.

The field production curves are shown in Figure 16. As illustrated in this figure, the TP13-A Sand reservoir oil production rate has varied from a maximum of 2,500 BOPD in August, 1971, to a low of 140 BOPD in April, 1982, with an average producing GOR of 880 SCF/STB, and 1,050 SCF/STB respectively. The increase in oil production rate up to an

Figure 5
Well A-1 Production History

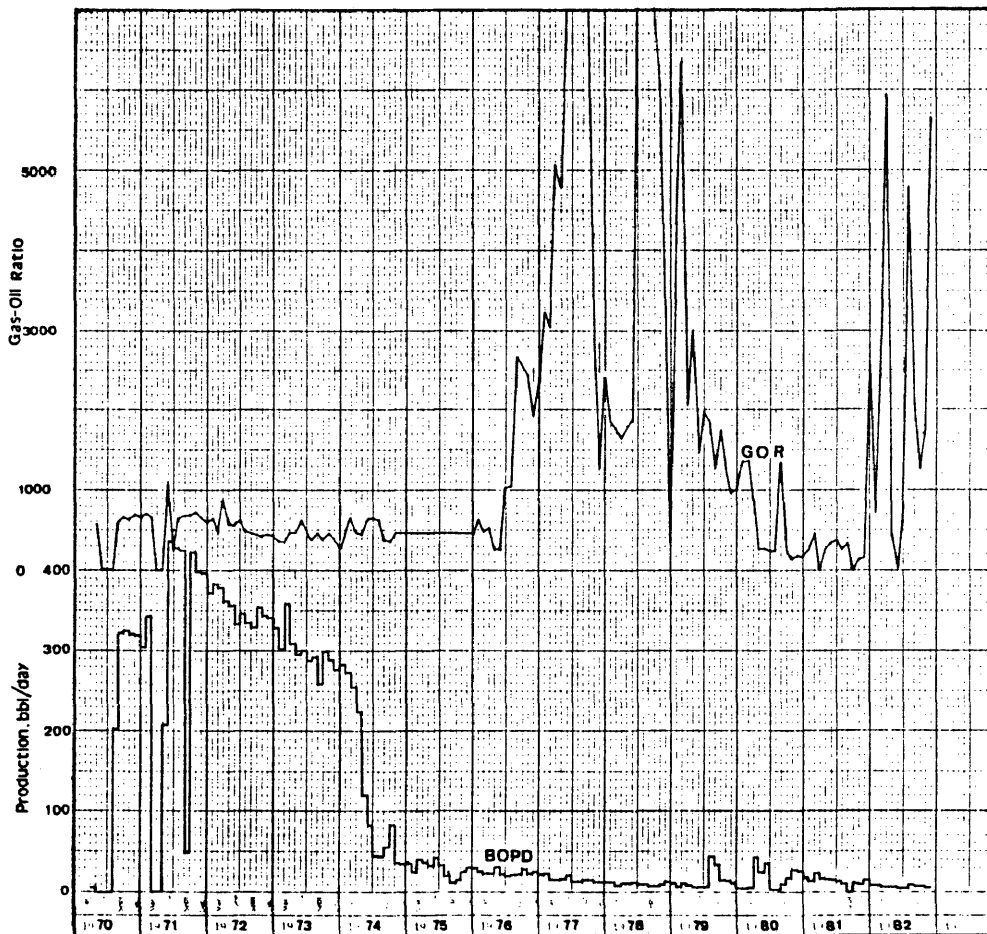


Figure 6
Well A-2 Production History

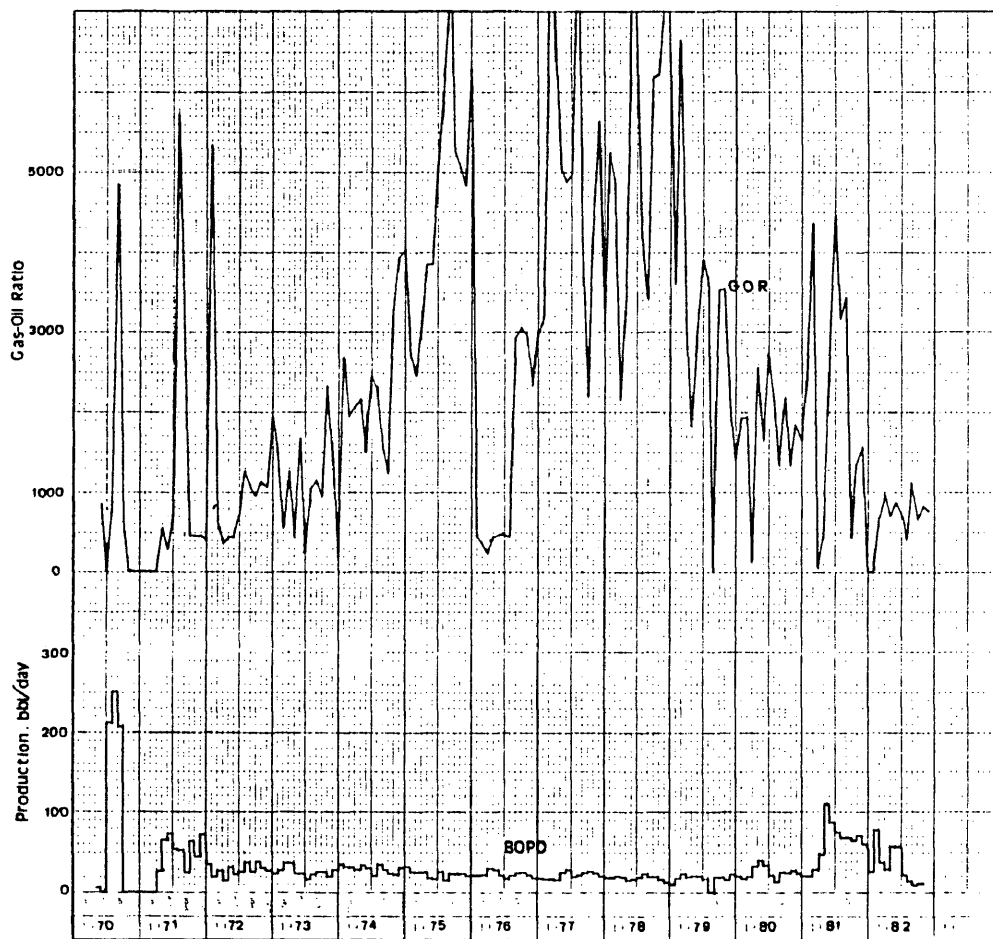


Figure 7
Well A-3 Production History

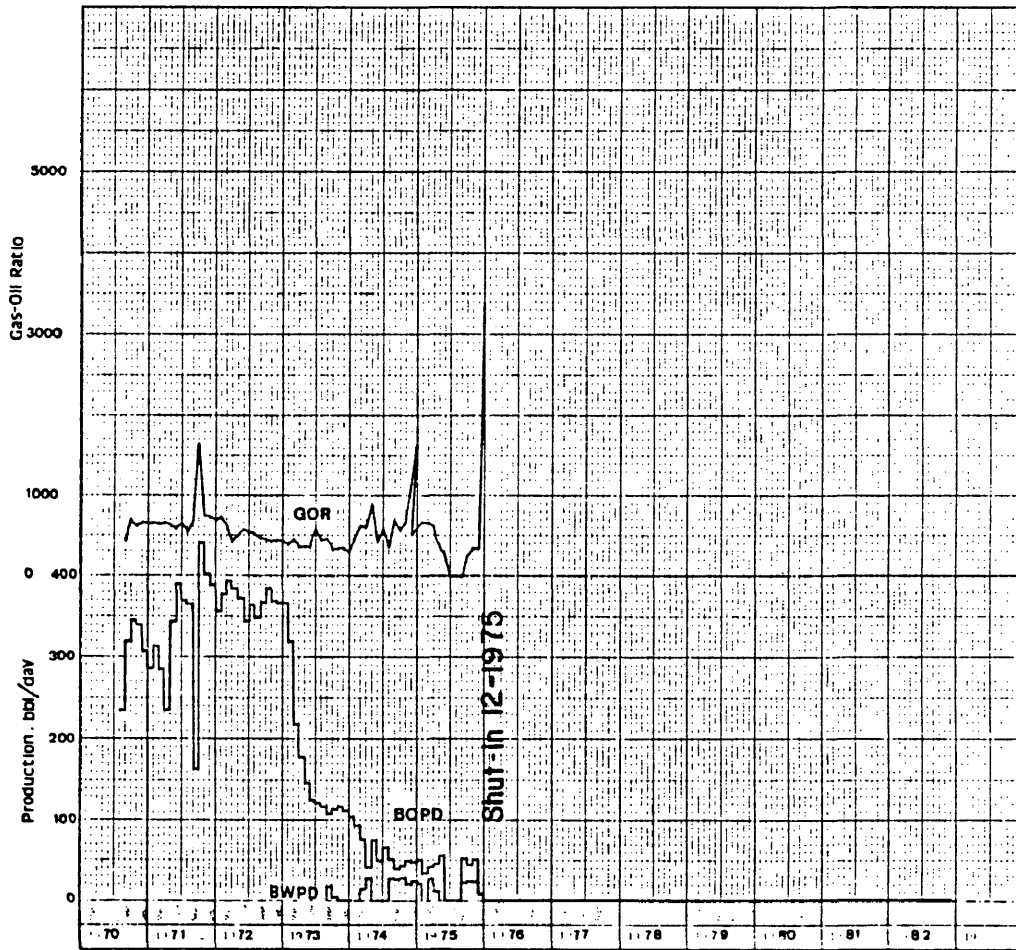


Figure 8
Well A-4 Production History

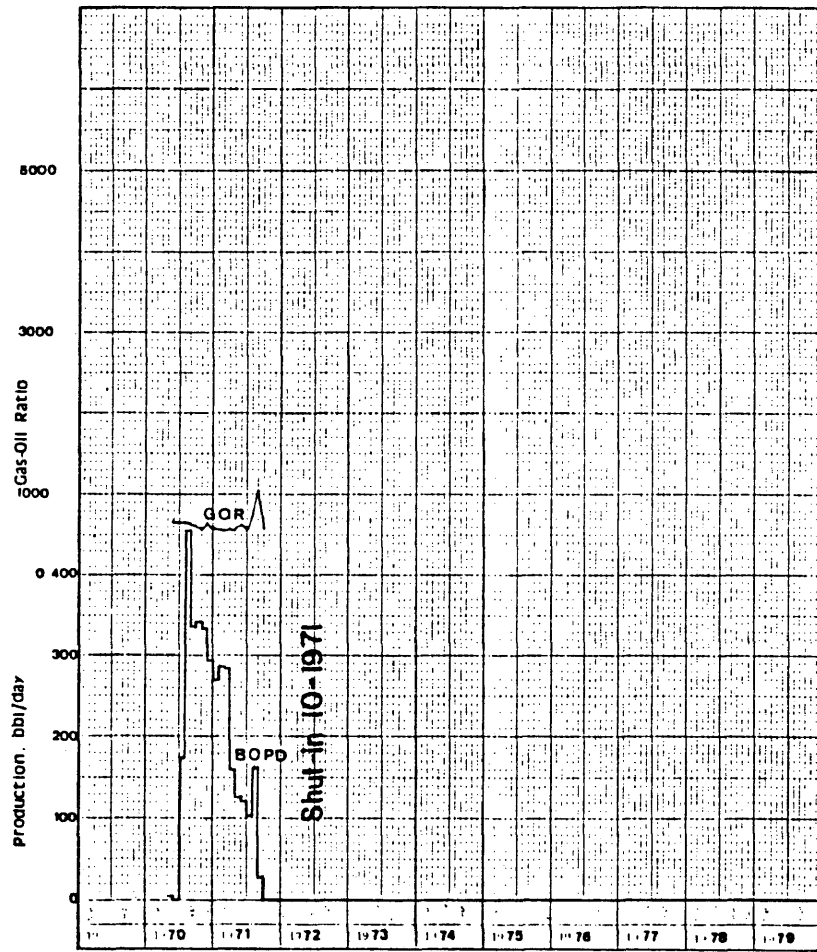


Figure 9
Well A-7 Production History

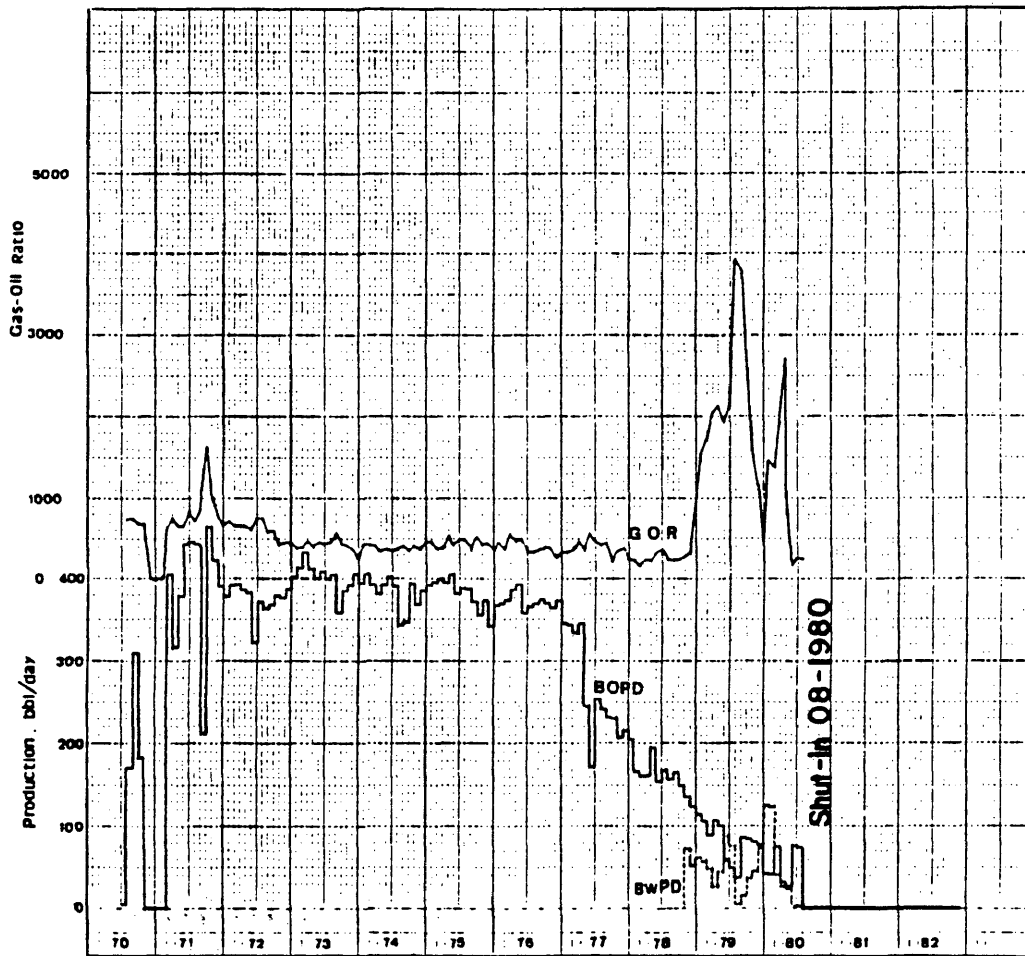


Figure 10
Well A-9 Production History

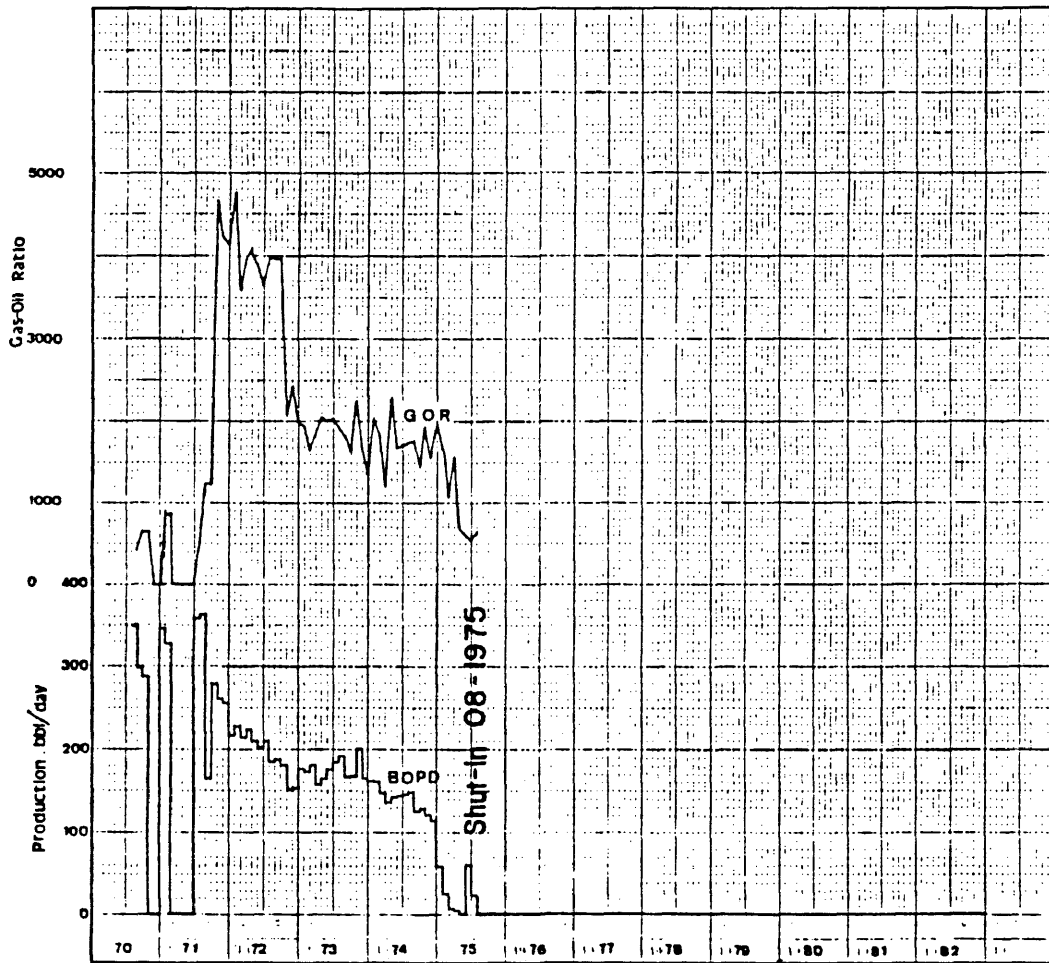


Figure 11
Well A-11 Production History

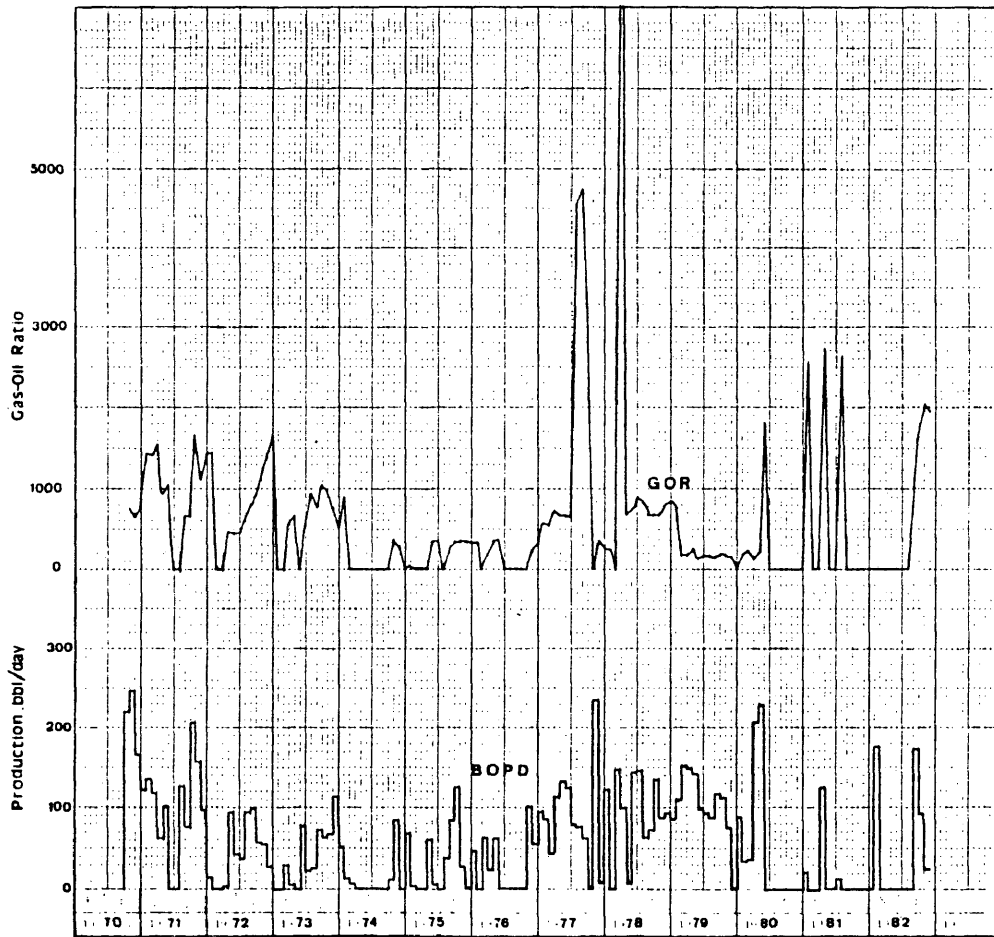


Figure 12
Well A-16 Production History

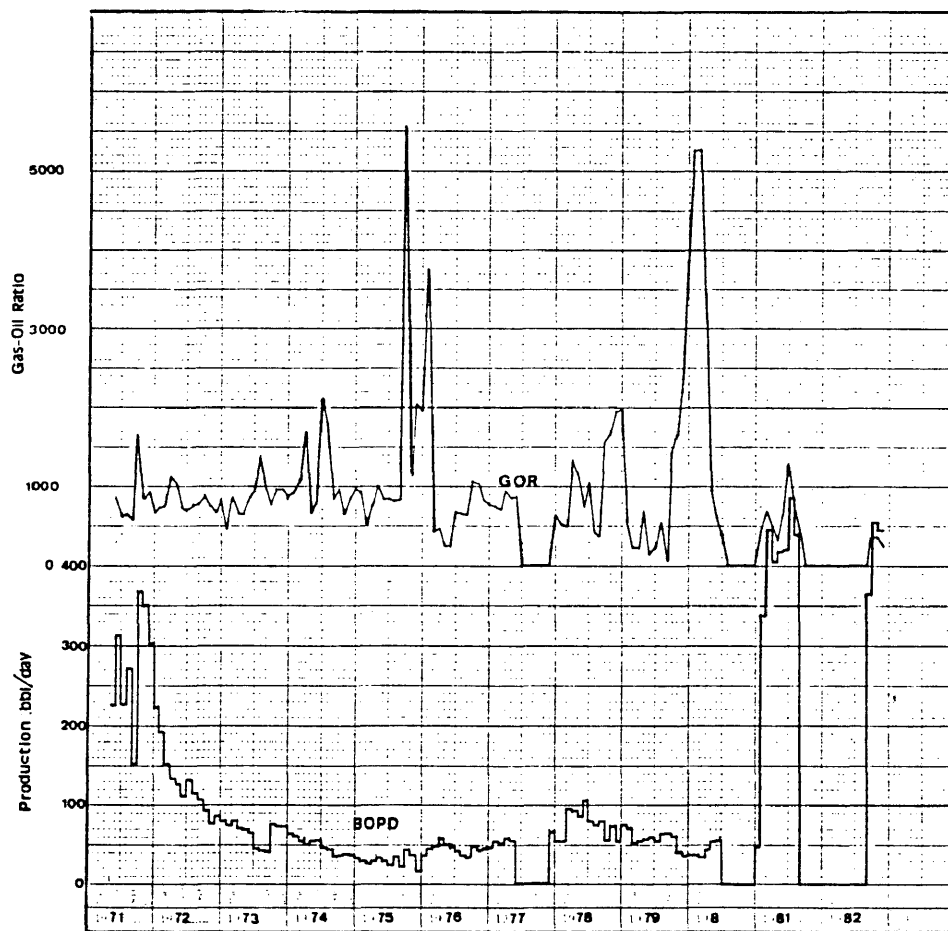


Figure 13
Well A-17 Production History

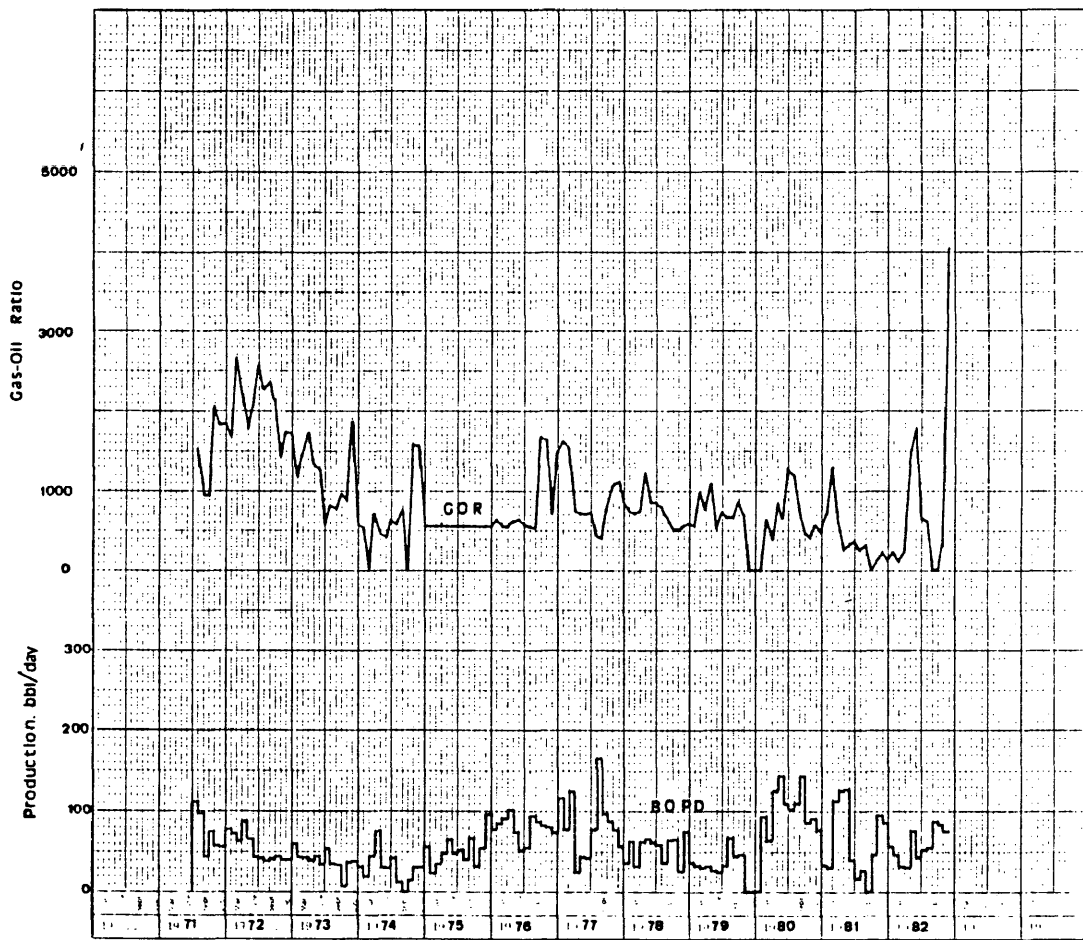


Figure 14
Well A-19 Production History

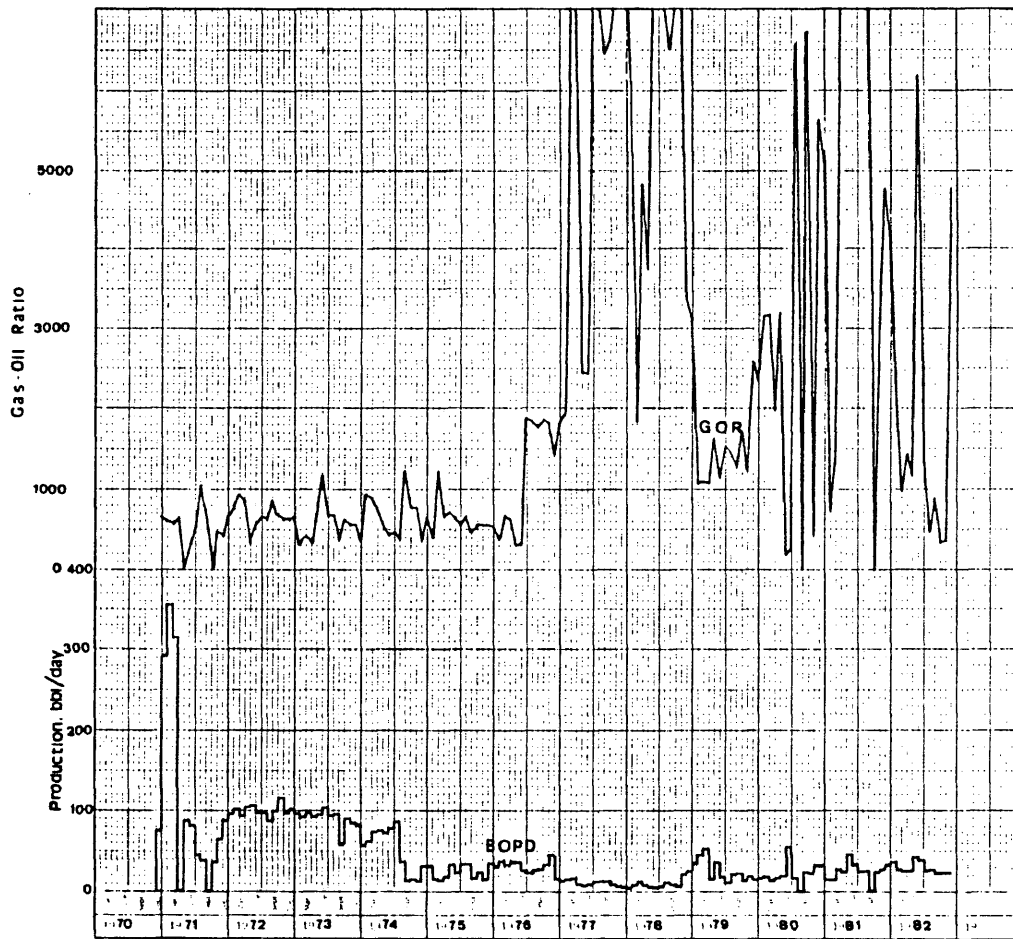


Figure 15
Well A-20 Production History

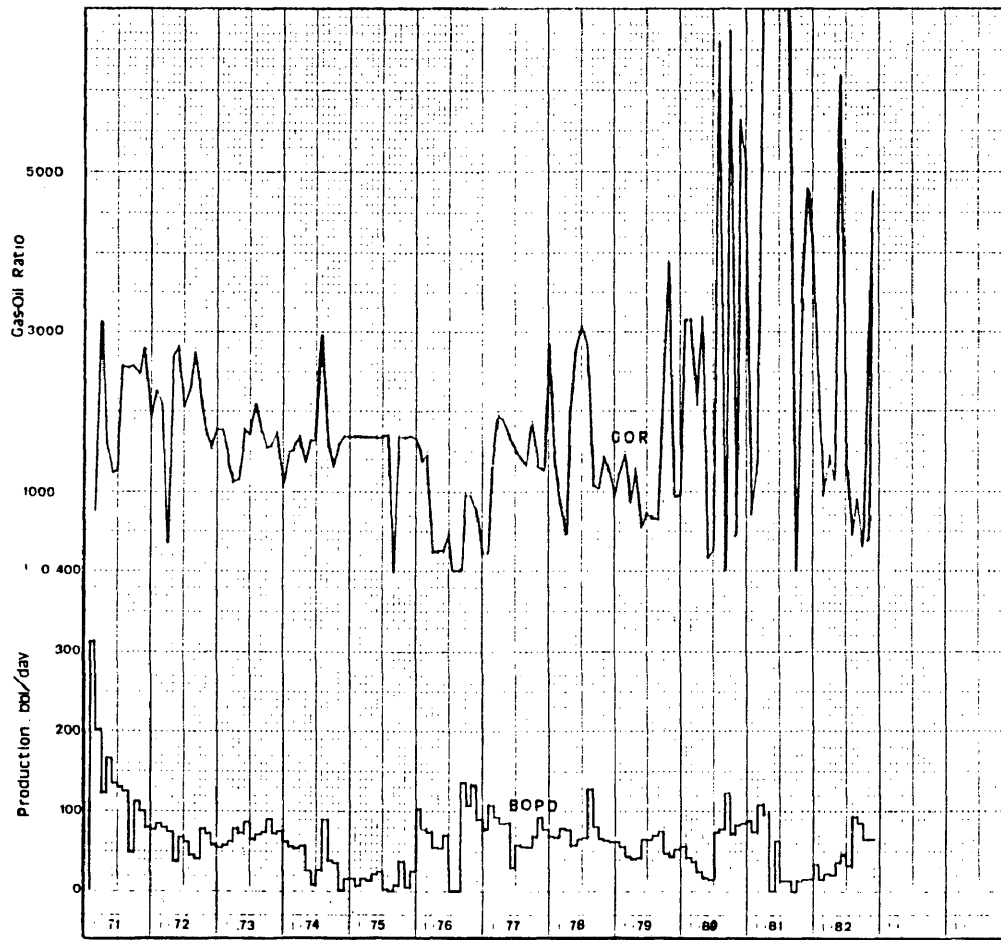
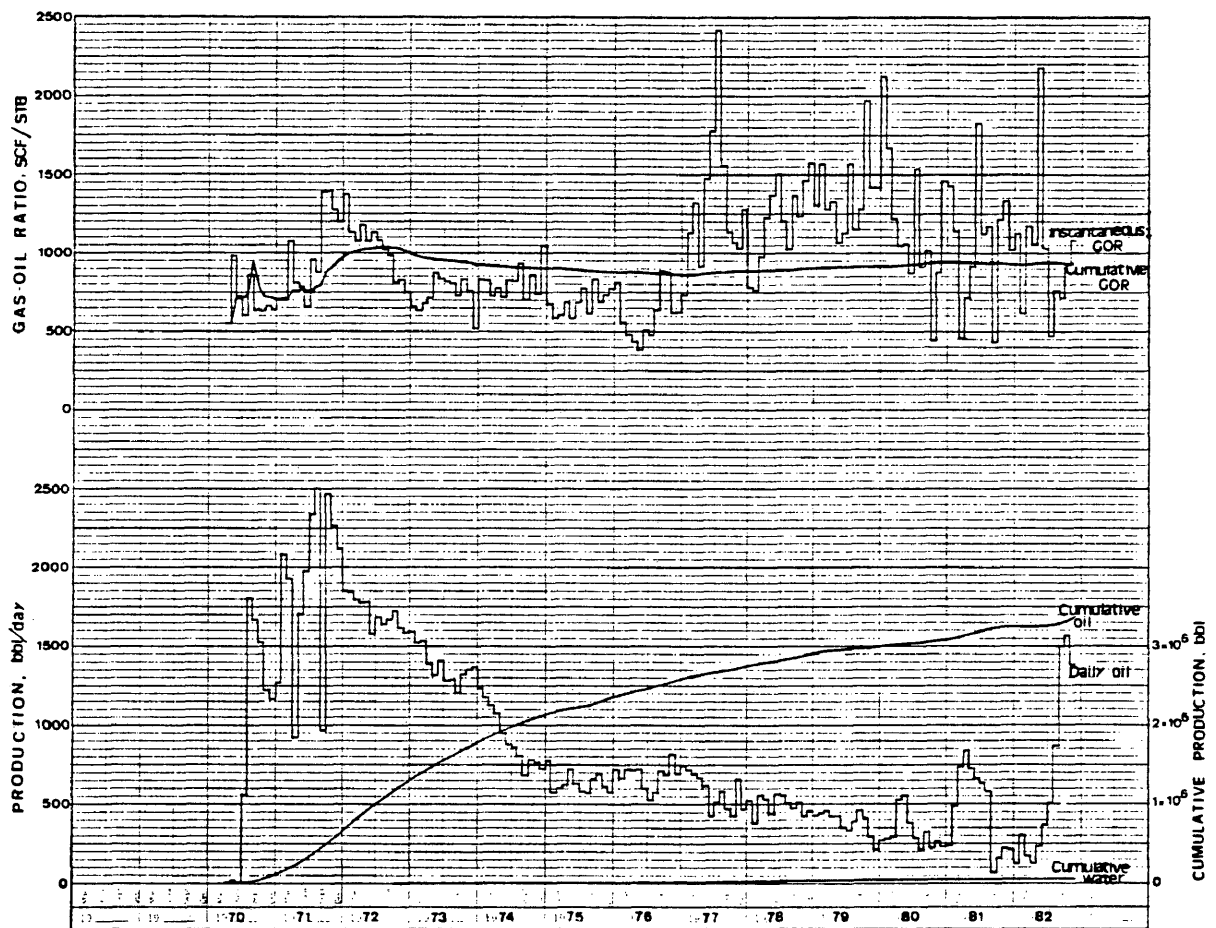


Figure 16
Field Production Curves



average of 1,500 BOPD in the last months of 1982, is mainly due to the completion of three infill wells.

This field is currently being produced by 10 wells. As of November, 1982, the field cumulative production amounted to 3,395,039 STB oil, 3,176,152 MSCF gas and 58,286 bbl water.

The maximum gas-oil ratio for the TP13-A Sand reservoir reached in July, 1977, was 2,400 SCF/STB as shown in Figure 16. Since that time, there has been a gradual reduction in gas-oil ratio to the most recent value of 1,060 SCF/STB. The original solution ratio was 673 SCF/STB at a saturation pressure of 3,631 psi.

The gas-oil ratio performance during the period January, 1973, to December, 1976, was relatively constant at somewhat reduced value.

The first significant water production occurred in 1974 in well A-3, and in 1977 in well A-7. These two wells were watered out and shut-in in 1975 and 1980, with a cumulative water production of 10,550 bbl and 42,899 bbl respectively.

It is believed that these wells were affected by mechanical problems rather than water encroachment, due to the fact that well A-7 produced water before the lower structure wells A-19 and A-1. With the exception of wells A-3, and A-7, water production has not been serious.

RESERVOIR PARAMETERS

A summary of the average reservoir rock and fluid properties is presented in Table 1. The following section briefly discusses how these parameters were estimated.

RESERVOIR ROCK PROPERTIES

Porosity

From an analysis of cores from 13 wells, with 112 core samples, values of median porosity, and arithmetic mean porosity were determined.

The arithmetic mean porosity was calculated from the equation:

$$\phi_a = \sum_i^n \phi_i * F_i$$

where: ϕ_a = arithmetic mean porosity, fractional

i = class mark of i -th class interval or range

ϕ_n = number of class intervals

F_i = frequency for i -th class interval, fractional

Table 2 shows the classification of porosity data, as well as the arithmetic mean porosity value calculated using the above equation. The value was found to be 27.7 percent. Figure 17 is a porosity histogram and distribution for all

TABLE 1
Summary Of The Average Reservoir Properties

ROCK PROPERTIES

Porosity, percent	27
Permeability, md	246
Connate water saturation, percent	36
Average thickness, ft	23
Average depth, ft	7,500

FLUID PROPERTIES

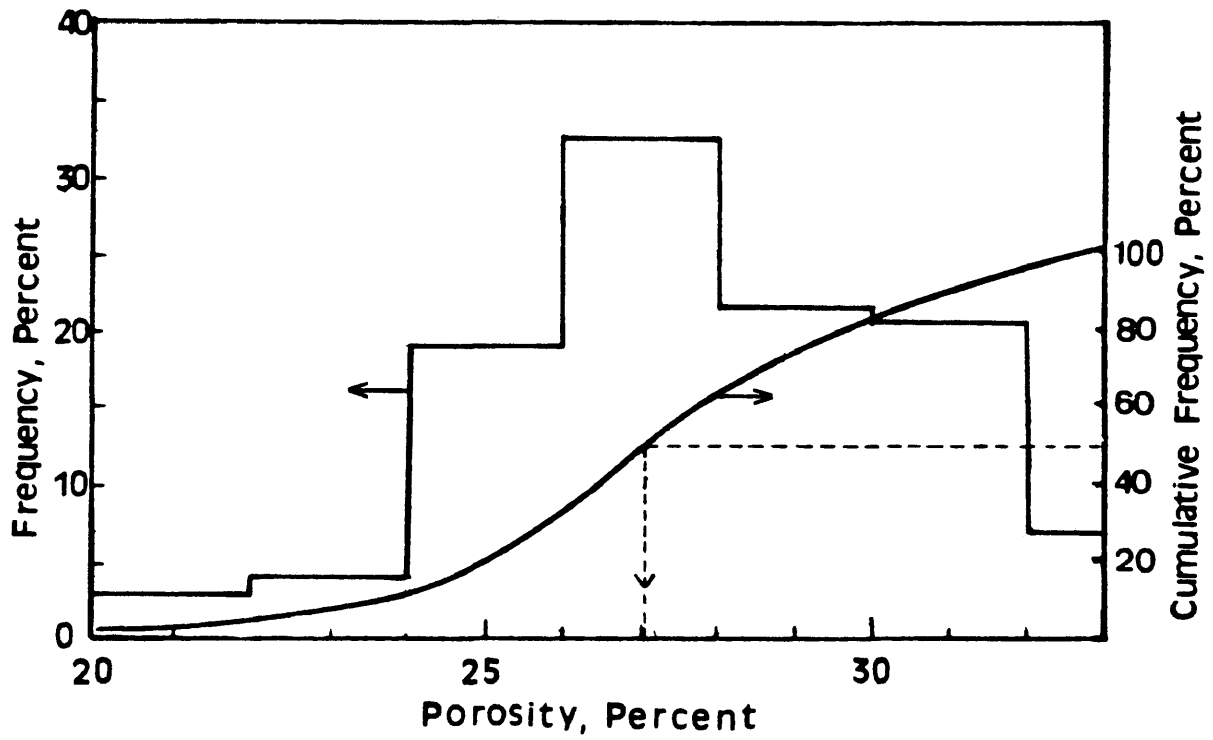
Reservoir temperature, deg F	154
Initial reservoir pressure a 7,500 ft, psi	3,631
Initial solution gas-oil ratio, scf/STB	673
Oil formation volume factor at bubble point pressure, bbl/STB	1.382
Viscosity at bubble point, cp	0.648
Gravity of stock-tank oil, deg API	35
Gas specific gravity, (air=1)	0.601

TABLE 2
Classification Of Porosity Data

Porosity Range %	Mid-value of Range ϕ_i	Number of Samples	Frequency Fraction F_i	$\phi_i * F_i$
Less than 20	19	3	0.0268	0.5089
20-22	21	3	0.0268	0.5625
22-24	23	2	0.0179	0.4107
24-26	25	21	0.1875	4.6875
26-28	27	33	0.2946	7.9554
28-30	29	22	0.1964	5.6964
30-32	31	21	0.1875	5.8125
32-34	33	7	0.0625	2.0625

Arithmetic mean porosity = $\phi_i * F_i = 27.7$

Figure 17
Porosity Histogram For Samples Of TP13-A Sand



samples from TP13-A Sand. From this figure, the value of median porosity was found to be 27.0 percent.

Porosity was also calculated from neutron-density logs, which were available for three infill wells drilled in 1982. The following equation was applied (Davis, 1982):

$$\phi_e = \phi_d - V_{sh} * \phi_{dsh}$$

where: ϕ_e = effective porosity

ϕ_d = density porosity

ϕ_{dsh} = density porosity in shale

V_{sh} = shale fraction

The shale fraction, V_{sh} , was determined by the following equation:

$$V_{sh} = \frac{\phi_n - \phi_d}{\phi_{nsh} - \phi_{dsh}}$$

where: ϕ_n = neutron porosity

ϕ_{nsh} = neutron porosity in shale

The calculated arithmetic mean porosity, weighted for thickness, from the wells C-1, C-3, and C-4 was found to be 26.3 percent. This value verifies the median porosity value of 27.0 percent used for all the calculations in the present study.

Permeability

Using the same cores used for evaluation of porosity, the arithmetic and geometric mean permeability were deter-

mined by statistical analysis (Amyx, et al., 1960).

The geometric mean permeability was calculated from the equation:

$$\log K_g = \sum F_j \log (K_a)_j$$

where: K_g = geometric mean permeability, millidarcies (md)

F_j = cumulative frequency of j interval, fractional

$(K_a)_j$ = arithmetic average permeability of logarithmic class interval j

n = total number of classified intervals

Table 3 shows the calculation of geometric mean permeability which was found to be 246 md. The arithmetic average permeability was 339 md. This good value of permeability plays very significant role in contributing to primary recovery, since together with the high degree of structural relief and the low oil viscosity of TP13-A Sand reservoir, make oil and gravity segregation particularly effective.

Connate Water Saturation

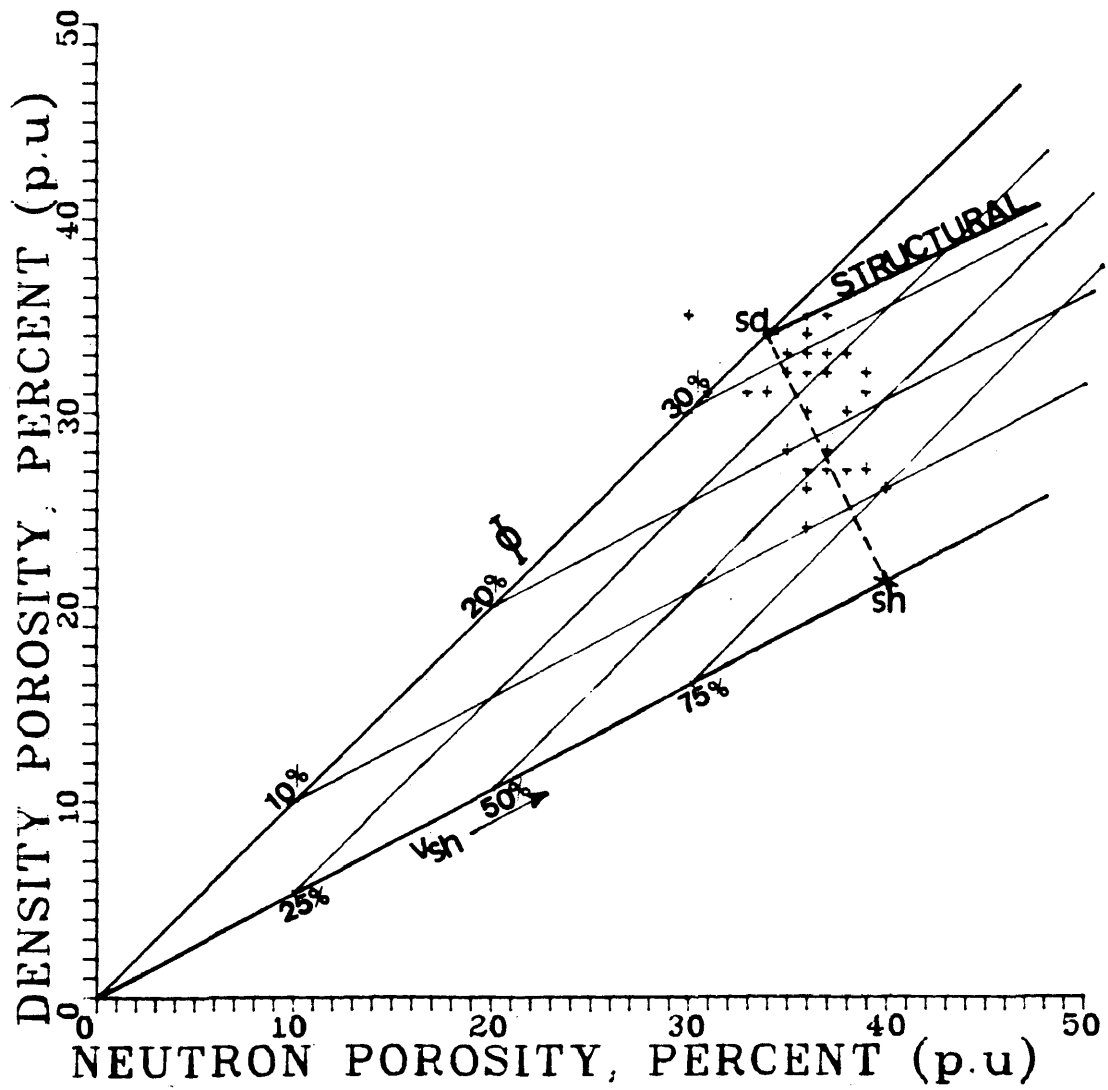
Shaly-sand evaluation was performed assuming that the formation contains either laminar or structural shale. This assumption is based on the results obtained from Figure 18, which is a neutron-density frequency cross plot. As shown in this figure, most of the plotted points fall on the Sd-Sh line or to the right of the line. This is an indication that the shale present is laminar and mainly structural.

TABLE 3
Calculation Of Geometric Mean Permeability

Perm. Range md.	Average Perm.of Range (Ka) j	Number of Samples	Frequency Fraction Fj	Cunulative Frequency	Fj* log (Ka) j
10.1-20	15	2	0.0179	0.0179	0.0210
20.1-40	30	4	0.0357	0.0536	0.0528
40.1-80	60	7	0.0625	0.1161	0.1111
80.1-160	120	20	0.1786	0.2946	0.3713
160.1-320	240	39	0.3482	0.6429	0.8288
320.1-640	480	26	0.2321	0.8750	0.6224
640.1-1280	960	10	0.0893	0.9643	0.2663
1280.1-2560	1920	4	0.0357	1.0000	0.1173
		112			2.3910

Geometric mean permeability = antilog 2.3910 = 246 md.

Figure 18
Neutron-Density Frequency Cross-Plot



The average water saturation for TP13-A Sand was determined from Simandoux equation (Davis, 1982):

$$\frac{1}{R_t} = \frac{S_w^2}{F \cdot R_w \cdot (1 - V_{sh})} + \frac{S_w \cdot V_{sh}}{R_{sh}}$$

where: S_w = water saturation

$$F = a \cdot \phi^{-m}$$

$$a = 0.81$$

$$m = 2.0, \text{ cementation factor}$$

R_w = resistivity of the virgin formation water, ohm-m.

V_{sh} = shale fraction

R_{sh} = shale resistivity, ohm-m.

Formation water resistivity, R_w , was estimated from well No.2 located in the southeast portion of Ship Shoal Area Block 229 (Figure 2, Region 3). This well penetrates the water oil contact.

An apparent water resistivity of 0.037 ohm-m was calculated from a water zone in well No.2 using the Archie equation. The average porosity was used in this calculation. Using this resistivity value, initial water saturations comparable to those reported in the literature (Frick, 1962 and Franklin, et al., 1975) for Miocene sands of Louisiana Gulf Coast, were calculated from induction and porosity logs available for the wells C-1, C-3, and C-4.

An average initial water saturation, weighted by pore volume, of 36.0 percent was obtained from wells C-1, C-3, and C-4. Table 4 shows an example of log calculation.

Effective Pay Thickness

This parameter was determined for each well from the induction, and spontaneous-potential logs. Core analysis was also helpful in making the determination. No porosity cut-off was used since porosity values within the gross interval were always above 18 percent.

TP13-A Sand thickness varied from 17 feet in well A-9, to 53 feet in well A-16. The average pay thickness for the sand was determined to be 23 feet.

RESERVOIR FLUID PROPERTIES

Laboratory analysis of the original reservoir fluids was not available; however, the presence of an initial gas-cap indicates an initially saturated reservoir. The reservoir fluid characteristics were calculated based on reservoir performance and published correlations.

The following equations were used to determine the solution gas-oil ratio, R_s , and the formation volume factor, B_o (Vazques and Beggs, 1980):

TABLE 4
Example Log Calculations, Well C-1

Depth	Rt	ϕ_D	ϕ_N	Vsh	ϕ_e	Sw
7190-91	2.4	34	36	0.10	32	0.32
91-92	3.6	34	36	0.10	32	0.26
92-93	4.4	33	36	0.14	30	0.24
93-94	4.0	33	36	0.14	30	0.24
94-95	2.4	31	33	0.10	29	0.35
95-96	1.9	26	36	0.48	16	0.39
7224-25	1.4	34	34	0.00	34	0.44
25-26	1.7	35	30	0.00	35	0.39
26-27	1.5	31	31	0.00	31	0.46
27-28	1.3	24	36	0.57		
7230-31	2.3	33	35	0.10	31	0.34
31-32	2.3	34	34	0.00	34	0.34
32-33	2.0	33	35	0.10	31	0.36
33-34	1.5	27	36	0.43	18	0.44
7241-42	2.0	34	34	0.00	34	0.31
42-43	3.4	34	35	0.10	32	0.28
43-44	3.9	35	36	0.05	34	0.25
44-45	3.2	34	36	0.10	32	0.27
45-46	2.1	34	34	0.00	34	0.36
46-47	1.4	30	38	0.38	22	0.43
50-51	1.2	28	35	0.33	21	0.51
7264-65	1.2	28	37	0.43	19	0.49
65-66	1.4	30	38	0.38	22	0.43
66-67	1.5	31	39	0.38	23	0.40
67-68	1.4	27	39	0.57	15	0.44
7294-95	1.3	30	36	0.29	24	0.46
95-96	2.0	32	37	0.24	27	0.35
96-97	2.6	34	36	0.10	32	0.31
97-98	2.6	35	37	0.10	33	0.30
98-99	2.3	34	36	0.10	32	0.33
99-00	1.8	32	36	0.19	28	0.38
7301-02	1.6	32	39	0.33	25	0.38
02-03	1.5	32	37	0.24	27	0.42
03-04	1.4	32	37	0.24	27	0.42

TABLE 4 (Continued)

Depth	Rt	ϕD	ϕN	Vsh	ϕe	Sw
7325-26	1.6	27	37	0.48	17	0.42
26-27	2.6	32	36	0.14	29	0.22
27-28	3.1	32	35	0.14	29	0.29
28-29	2.8	34	34	0.00	34	0.31
29-30	2.0	30	38	0.38	22	0.34
7366-67	1.2	27	38	0.52	16	
67-68	1.4	26	40	0.67	12	
68-69	1.5	33	38	0.24	28	0.40
69-70	1.3	33	37	0.19	29	0.44

$$R_{sh} = 0.7$$

$$R_w = 0.037$$

$$\phi N_{sh} = 42$$

$$\phi D_{sh} = 21$$

$$h = 41$$

$$\phi e = 28$$

$$Sw = 36.5$$

$$R_s = C_1 * (\gamma_{gs}) * (P)^{C_2} * \exp C_3 * (\gamma_o) / (T+460)$$

where: R_s = dissolved GOR, scf/STB

$$C_1 = 0.0178$$

$$C_2 = 1.1870$$

$$C_3 = 23.9310$$

γ_{gs} = gas gravity (air=1) that would result from separator conditions of 100 psig

P = pressure, psia

γ_o = oil gravity, API degrees

T = temperature, degrees F

$$B_o = 1 + C_1 * R_s + C_2 (T-60) (\gamma_o / \gamma_{gs}) + C_3 * R_s (T-60) (\gamma_o / \gamma_{gs})$$

where: B_o = oil FVF, bbl/STB

$$C_1 = 4.670 * 10^{-4}$$

$$C_2 = 1.100 * 10^{-5}$$

$$C_3 = 1.337 * 10^{-9}$$

Oil viscosity was calculated from the equation (Beggs and Robinson, 1975):

$$\mu_o = A * \mu_{oDB}$$

where: μ_o = viscosity of gas-saturated oil at T , cp

$$A = 10.715 (R_s + 100)^{-0.515}$$

$$B = 5.440 (R_s + 150)^{-0.338}$$

$$\begin{aligned} \mu_{OD} &= 10^x - 1 \\ x &= y \cdot T^{-1.163} \\ y &= 10^z \\ z &= 3.0324 - 0.02023 \cdot \gamma_o \\ \mu_{OD} &= \text{viscosity of gas-free oil at } T, \text{ cp} \end{aligned}$$

Figures 19 to 21 illustrate the solution gas-oil ratio; the oil formation volume factor; and the oil viscosity as a function of pressure.

The gas deviation factors for various pressures were calculated (Hall and Yarborough, 1964); they are shown in Figure 22.

The gas formation volume factor was evaluated from the equation:

$$B_g = \frac{0.00515 \cdot Z \cdot T}{P}$$

where: B_g = gas formation volume factor, Bbl/SCF
 Z = deviation factor
 T = reservoir temperature, degrees R
 P = reservoir pressure, psia

Figures 23 and 24 show a plot of gas formation volume factor and gas viscosity versus pressure, respectively.

Figure 19

Solution Gas-Oil Ratio vs Pressure

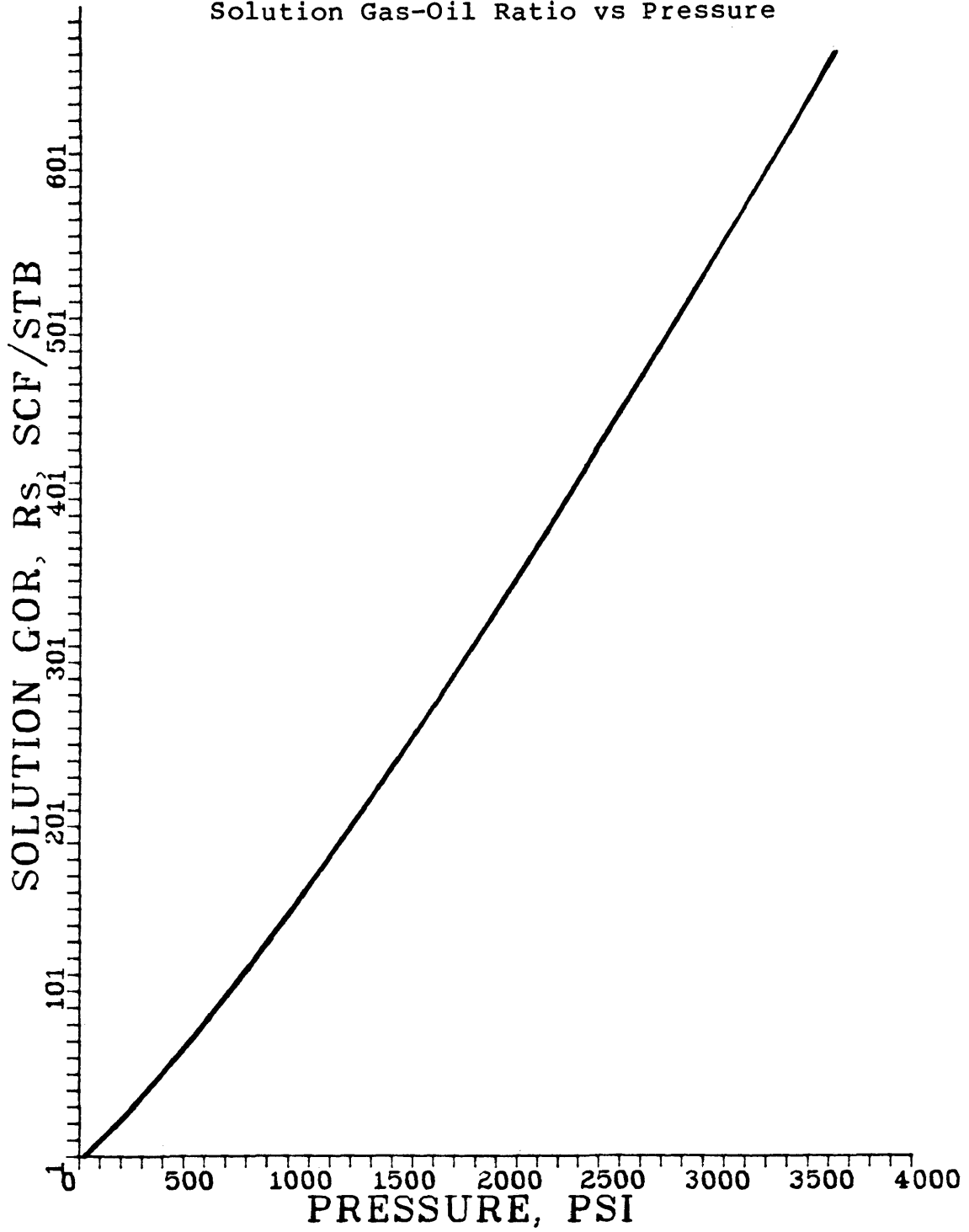


Figure 20

Oil Formation Volume Factor vs Pressure

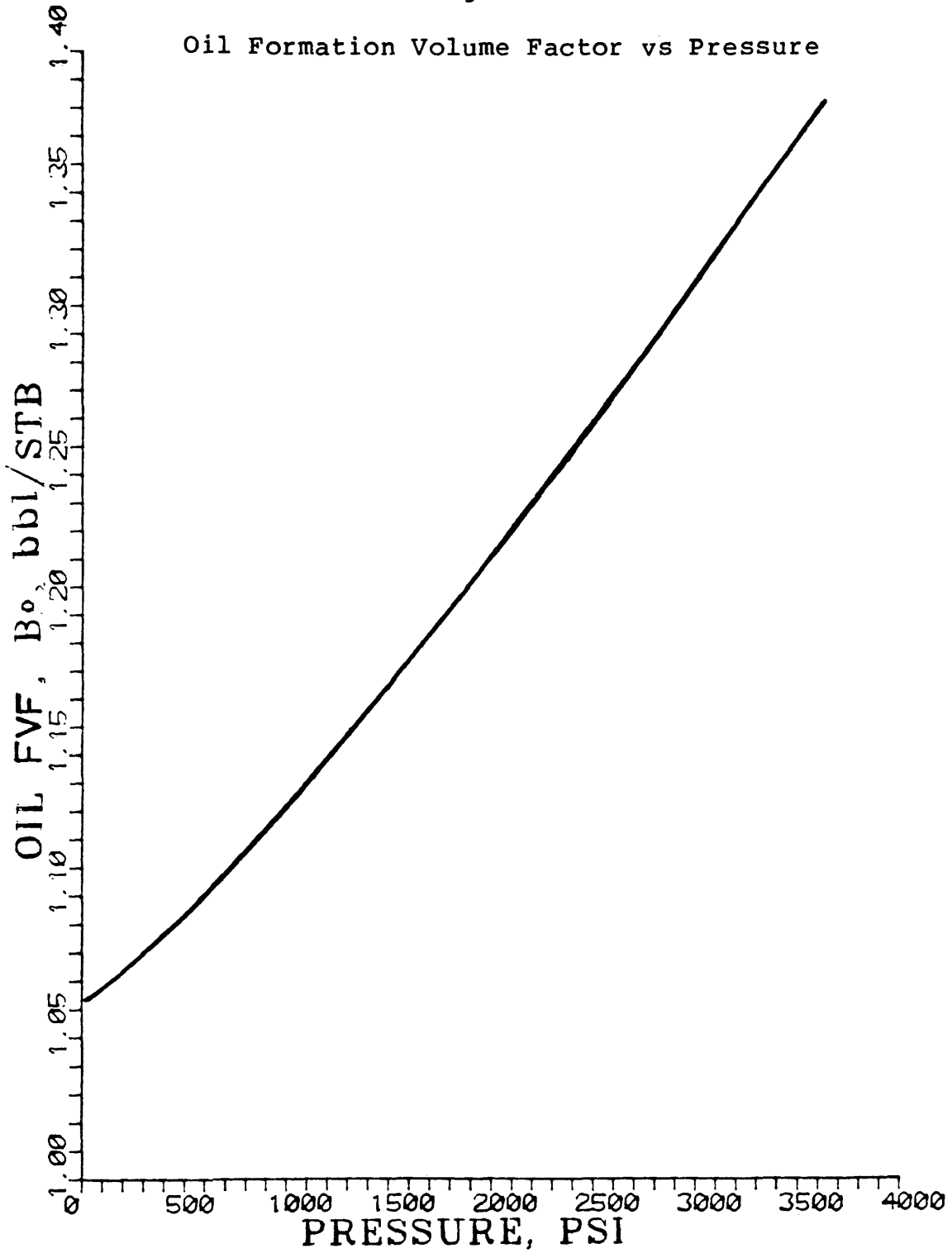


Figure 21

Oil Viscosity vs Pressure

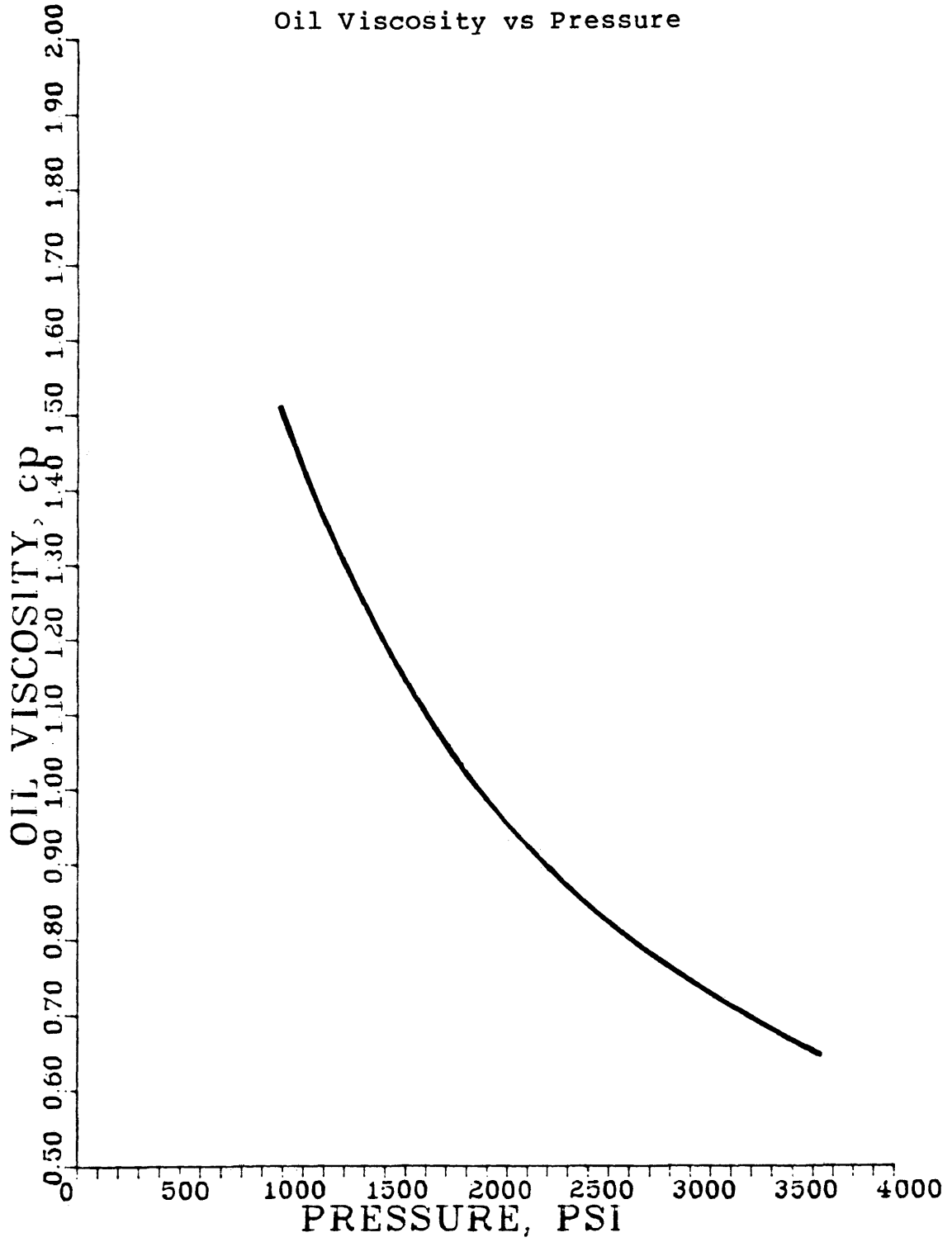


Figure 22

Gas Deviation Factor vs Pressure

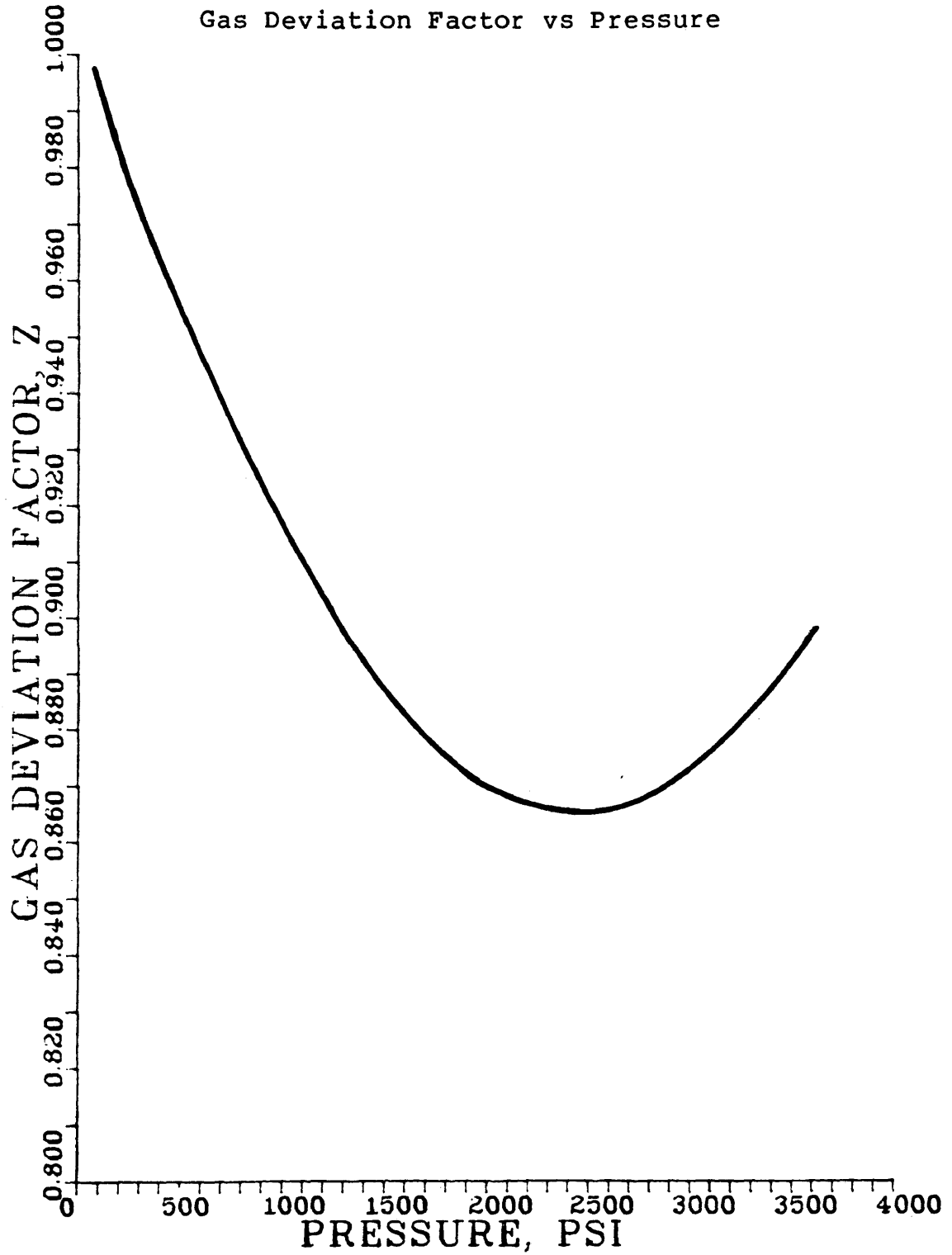


Figure 23

Gas Formation Volume Factor vs Pressure

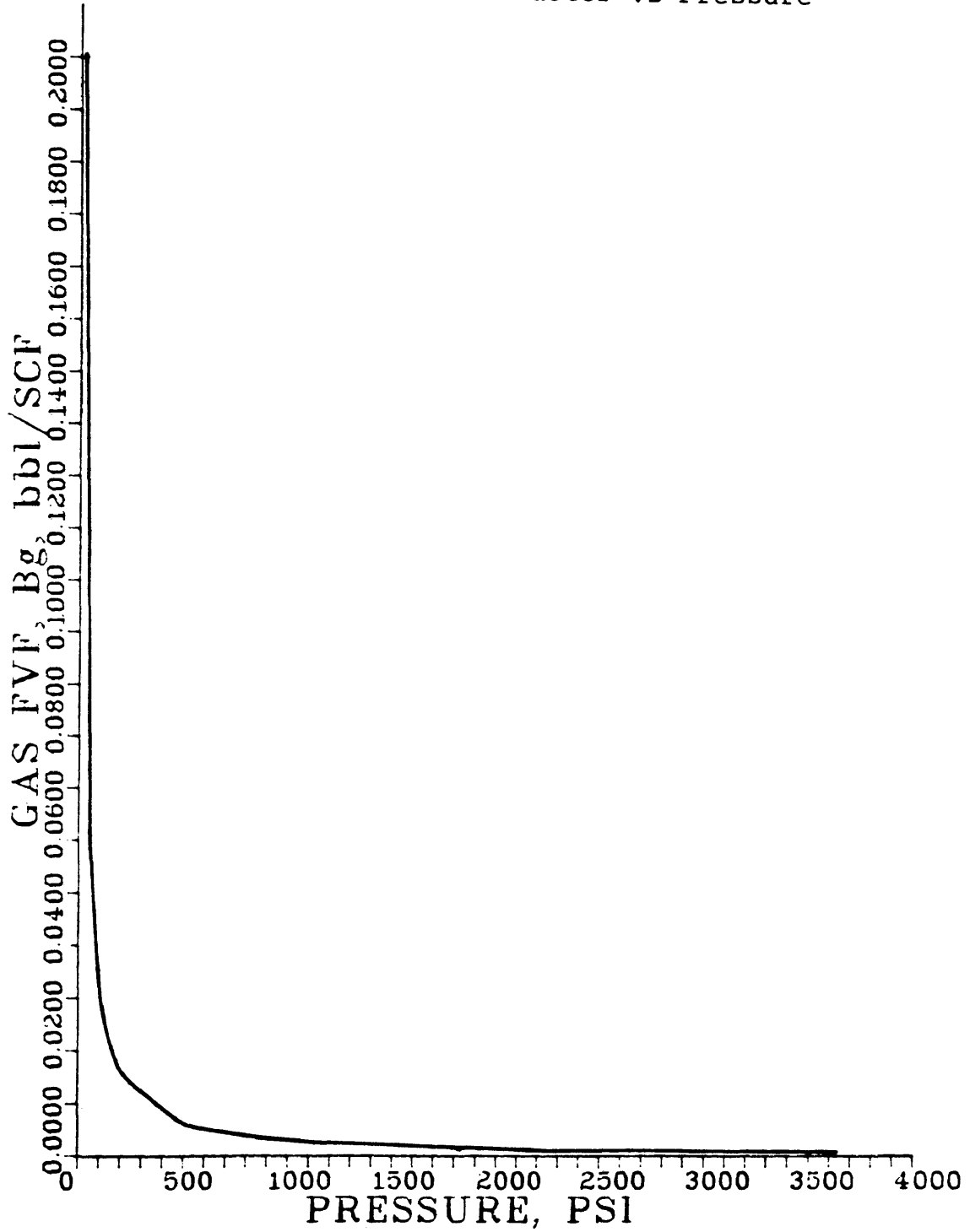
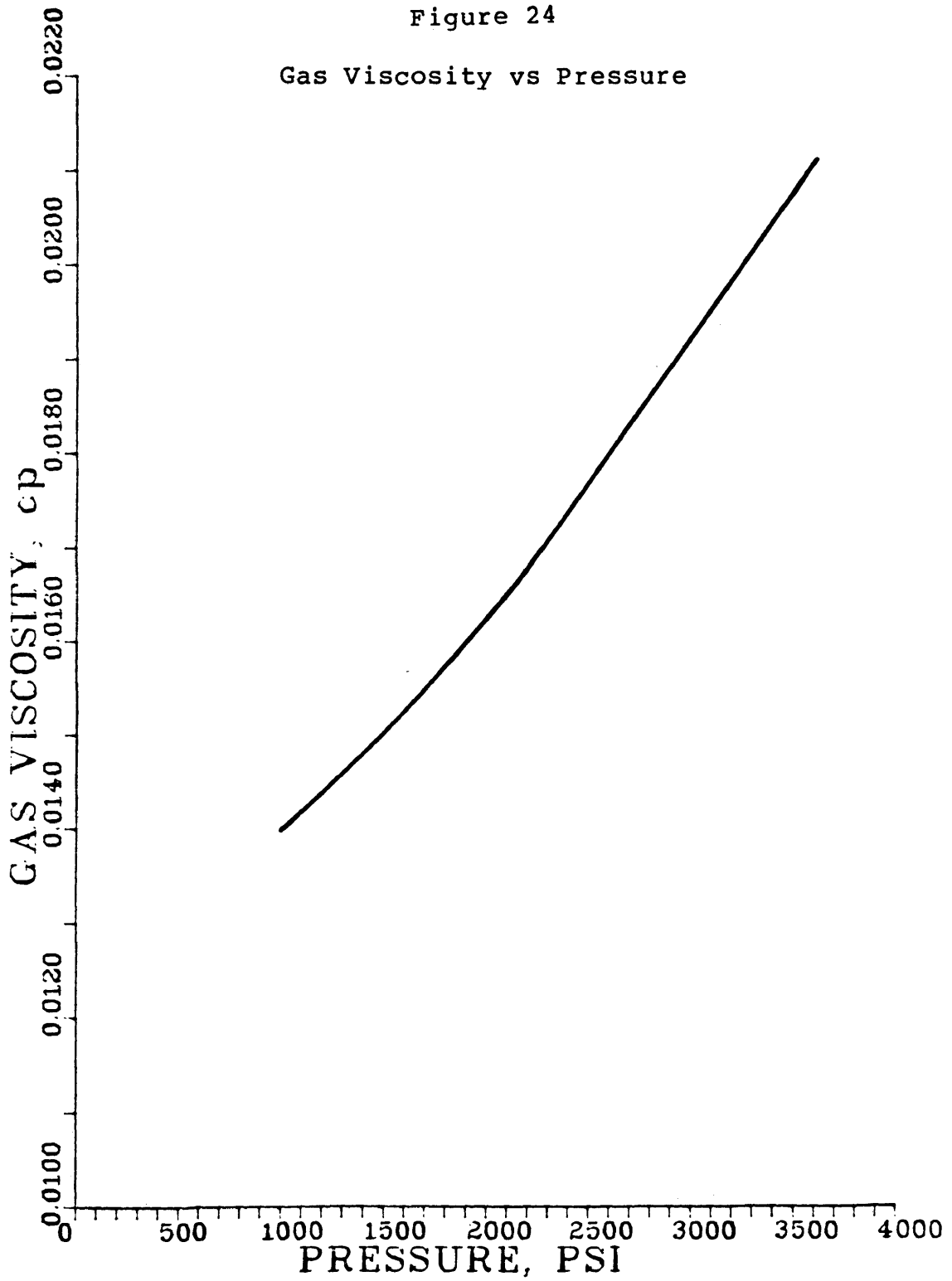


Figure 24
Gas Viscosity vs Pressure



VOLUMETRIC DETERMINATION OF ORIGINAL OIL-IN-PLACE

From structure maps drawn on the top and on the base of TP13-A sand (Figures 25 and 26), isopachous maps (Figure 4) of the net oil and net gas sand, contoured on 5 feet sand thickness were constructed (Bankhead and McCord, 1970). The sand count was based upon consideration of core data and electric logs.

A total net productive oil sand volume of 10,596 acre-ft was planimetered from the net pay isopachous map. The productive sand encompasses an area of 468 acres and has an average thickness of 23 feet.

Figure 27 shows the approximate structural distribution of the net oil productive sand volume as determined by superimposing the isopachous map upon the structure, and computing the sand volume between structure contours.

The size of the gas-cap is minor in relation to that of the oil reservoir. The net gas sand volume was calculated to be 206 acre-ft.

Tables 5 and 6 show the calculation of the net oil and net gas sand volumes from isopachous maps.

The original oil-in-place was obtained using the reservoir properties summarized in Table 1, and the following equation:

Figure 25
Top Of TP13-A Sand Structure Map

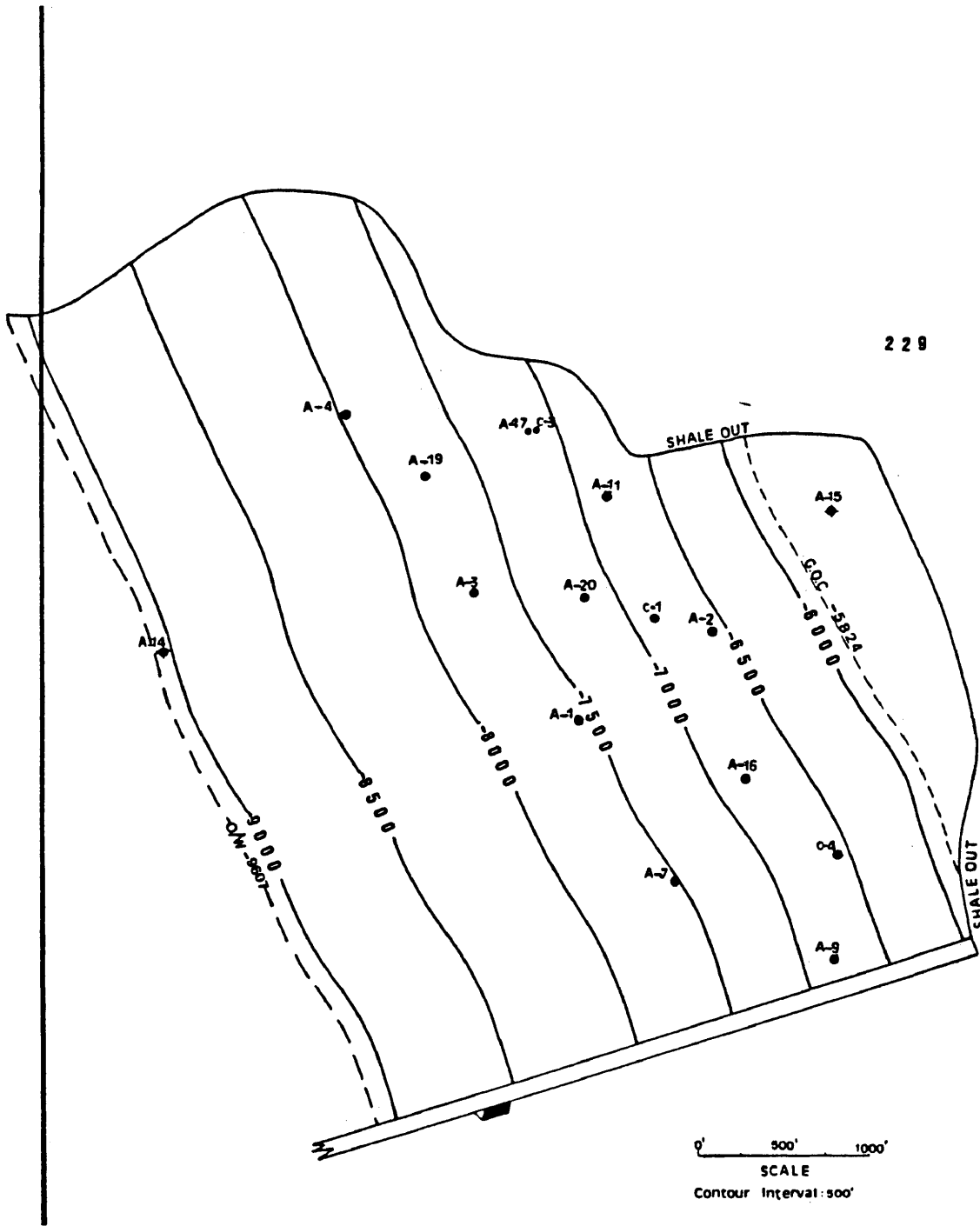


Figure 26
Bottom Of TP13-A Sand Structure Map

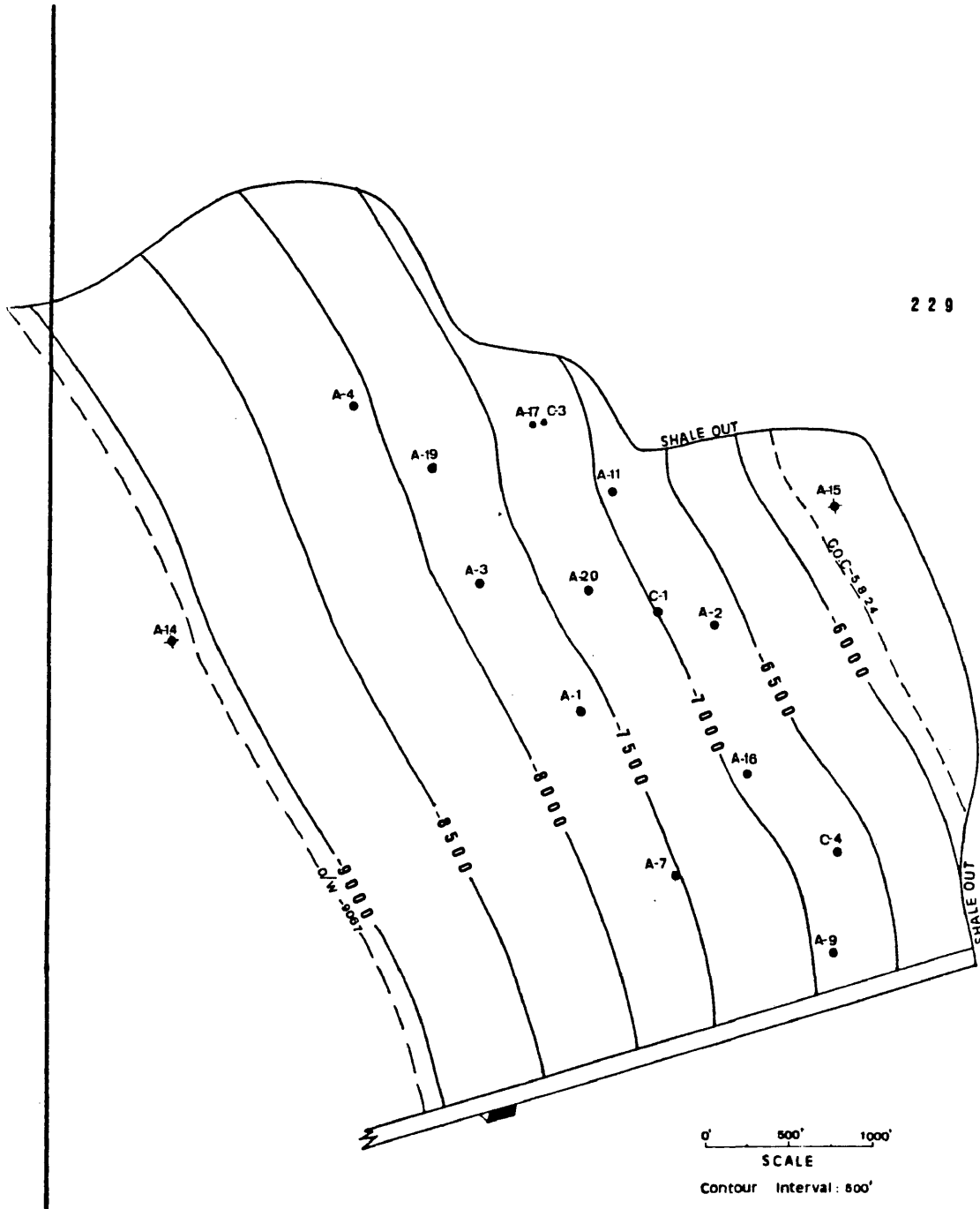


Figure 27
Structural Distribution Net Productive Sand

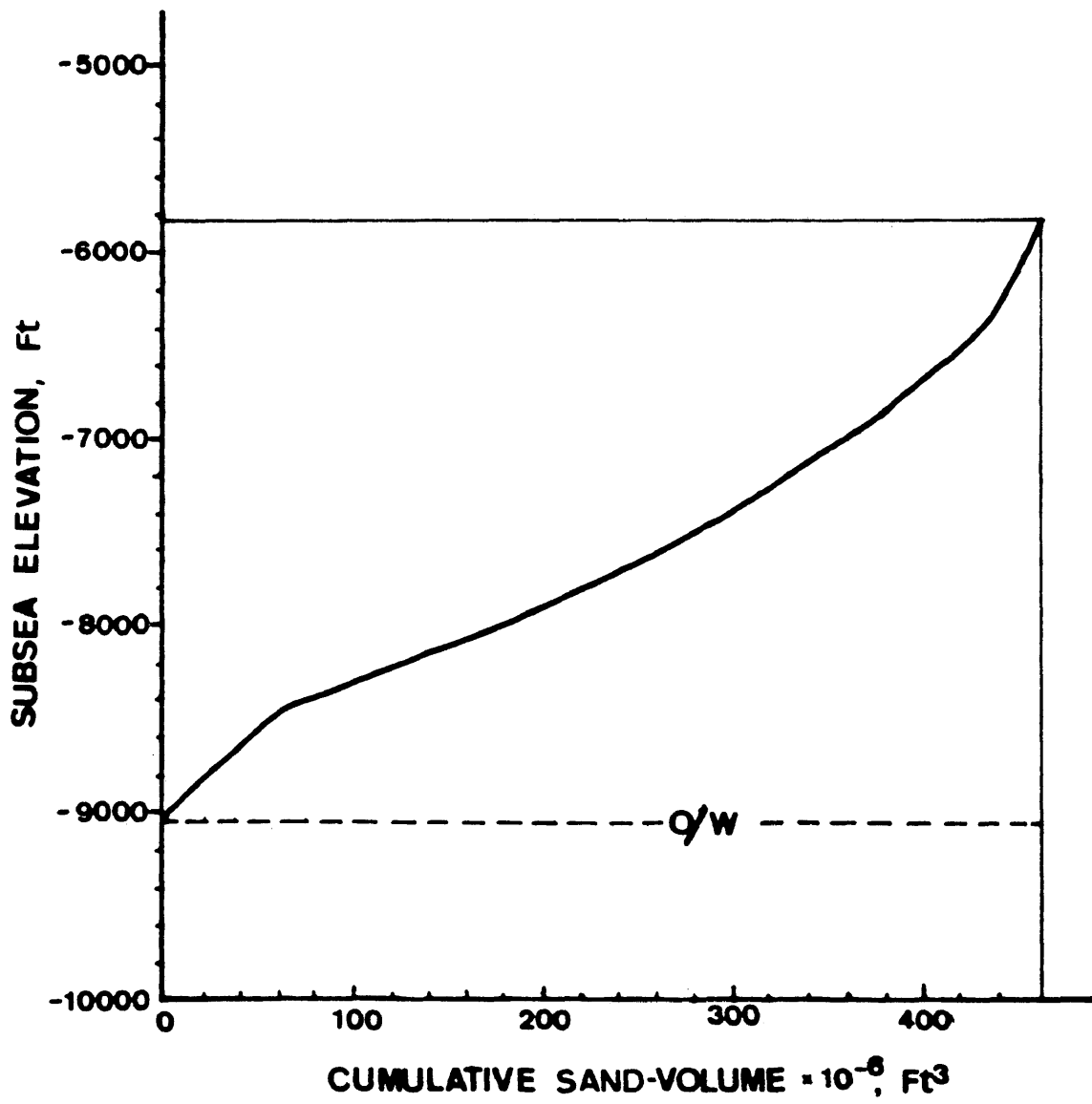


TABLE 5

Calculation Of Net Oil Sand Volume From Isopachous Map

Productive Area	Planimeter Reading*	Area Acres	Ratio Areas	Interval ft	Equation	V Acre-ft
0	4.080	468.3				
5	3.484	399.9	0.85	5	Trap	2,171
10	3.088	354.4	0.89	5	"	1,886
15	2.691	308.8	0.87	5	"	1,658
20	2.295	263.4	0.85	5	"	1,431
25	1.904	218.5	0.83	5	"	1,205
30	1.303	149.6	0.68	5	"	920
35	0.897	102.9	0.69	5	"	631
40	0.512	58.8	0.57	5	"	404
45	0.241	27.7	0.47	5	Pyr	211
50	0.044	5.1	0.18	5	"	74
	0.000	0.0	0.00	3	"	5
						10,596

* For a map scale of one inch = 500 ft

Constant: one square inch = 5.74 Acres

TABLE 6

Calculation Of Net Gas Sand Volume From Isopachous Map

Productive Area	Planimeter Reading*	Area Acres	Ratio Areas	Interval ft	Equation	V Acre-ft
0	0.1290	29.6				
5	0.0760	17.4	0.59	5	Trap	118
10	0.0360	8.3	0.48	5	"	63
15	0.0088	2.0	0.24	5	Pyr	24
	0.0000	0.0	0.00	1	"	1
						----- 206

* For a map scale of one inch = 500 ft

Constant: one square inch = 5.74 Acres

$$N = 7,758 * V * \phi * (1 - S_{wi}) / B_{oi}$$

where: N = stock-tank oil initially in-place, STB
 V = net bulk volume, acre-ft
 ϕ = porosity, fractional
 S_{wi} = average initial water saturation, fractional
 B_{oi} = oil formation volume factor at initial pressure, bbl/STB
 7,758 = conversion factor, Bbls/Acre-ft

The initial stock-tank oil-in-place was calculated to be 10.3 million bbl, or 970 STB per acre-ft.

The initial gas-in-place was estimated with the use of the following equation:

$$G = 43,560 * V * \phi * (1 - S_{wi}) / B_{gi}$$

where: G = original gas-in-place, SCF
 V = net bulk volume, acre-ft
 ϕ = porosity, fractional
 S_{wi} = average initial water saturation, fractional
 B_{gi} = gas formation volume factor at initial pressure, cu.ft/SCF
 43,560 = conversion factor, cu.ft/Acre-ft

The volumetrically estimated original free gas-in-place was 356 MMSCF.

Assuming the rock in the gas-cap and that of the oil

zone to be essentially the same, the ratio of the initial gas-cap volume to the initial oil volume is 0.02.

MATERIAL BALANCE
PAST PERFORMANCE CALCULATIONS

Input data for material balance calculations is shown in Table 7. The field performance history of the TP13-A Sand showing the daily oil production, cumulative oil and water production, and the instantaneous and cumulative GOR is presented in Figure 16.

The initial pressure recorded in the discovery well A-1 corrected at 7,500 feet subsea datum, was assumed as the original reservoir pressure. The average reservoir pressure at any time after initial production, was estimated from 24 hour bottom-hole shut-in pressures measured at various time intervals. These data are presented in Table 8.

Because of the large reservoir pressure gradient from north to south, a volumetric averaging technique was used to obtain the average reservoir pressure. Volumetric weighted pressures were determined by superimposing the isobaric map on an isopach map, and determining the sand volume between successive pressure contours (Amyx, et. al., 1960). Average reservoir pressure versus cumulative production, and versus time, are plotted in Figures 28 and 29 respectively.

P-V-T data was calculated from published correlations (Vasquez and Beggs, 1980).

The straight-line material balance method was used to

TABLE 7
Input Data For Material Balance Calculations

Date	BHP (psi)	CUMULATIVE		
		OIL (STB)	GAS (MSCF)	WATER (STB)
April, 1969	3,631			
Jun, 1970	3,610	546	388	0
Dec,	3,490	137,336	96,426	0
Jun, 1971	3,330	340,331	256,907	0
Dec,	3,260	675,035	652,604	0
Jun, 1972	3,230	997,876	1,028,768	0
Dec,	3,155	1,302,778	1,305,318	68
Jun, 1973	3,110	1,555,546	1,488,001	68
Dec,	3,094	1,795,851	1,666,849	875
Jun, 1974	3,040	1,990,484	1,820,195	2,110
Dec,	2,995	2,132,529	1,941,726	6,284
Jun, 1975	2,968	2,251,771	2,018,099	9,105
Dec,	2,935	2,365,165	2,101,641	11,359
Jun, 1976	2,907	2,480,382	2,164,319	11,547
Dec,	2,875	2,594,904	2,244,674	11,581
Jun, 1977	2,840	2,693,253	2,360,371	25,417
Dec,	2,807	2,772,079	2,474,231	25,522
Jun, 1978	2,783	2,841,968	2,551,884	25,742
Dec,	2,756	2,912,733	2,644,617	28,997
Jun, 1979	2,732	2,968,456	2,715,848	38,757
Dec,	2,715	3,012,874	2,841,441	45,191
Jun, 1980	2,700	3,061,083	2,876,801	55,292
Dec,	2,680	3,093,779	2,970,284	55,906
Jun, 1981	2,650	3,185,723	3,057,003	56,673
Dec,	2,634	3,231,999	3,176,152	57,896

TABLE 8

Bottom-Hole Pressure Data
(Datum = -7,500 feet)

Date	Well:	A-1	A-3	A-7	A-11	A-16	A-17	A-19	A-20
3-69		3,631							
11-70		3,545							
3-71			3,132						
5-71		3,457							
6-71								2,720	2,160
9-71						3,473			
11-73						3,300			
4-74			3,155		2,234	3,177			
9-75									2,440
11-75		3,014						2,680	
4-76					2,340				
4-77							2,420		
7-79		2,077		2,574			2,140	2,020	
7-80		3,040							
8-80				3,046				2,350	
9-80							2,283		
1-81								2,020	
4-81						3,030	2,305		
10-81							2,219		
11-81				3,064					
2-82				3,080					
9-82				3,043					
11-82						2,996			

Figure 28

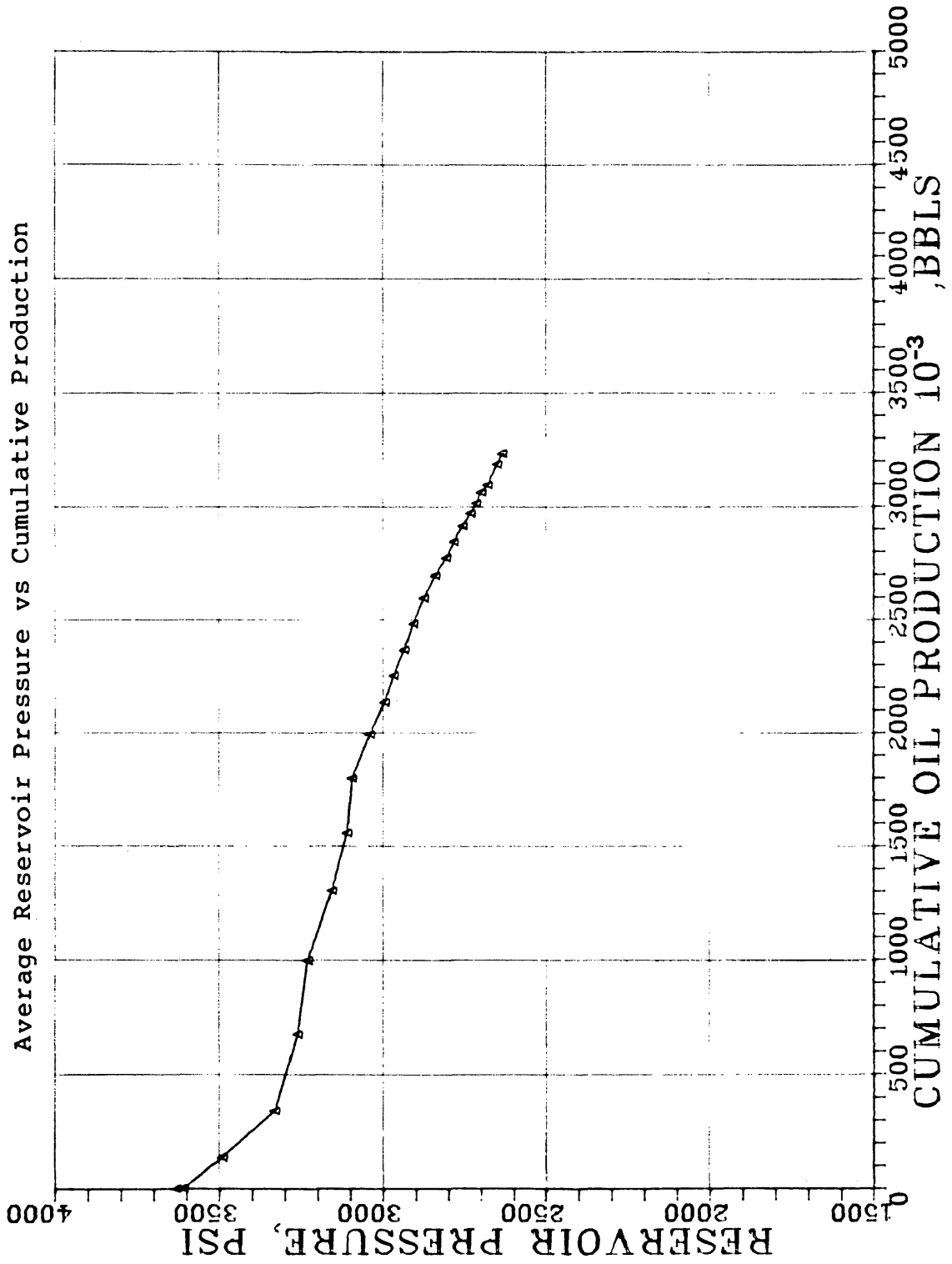
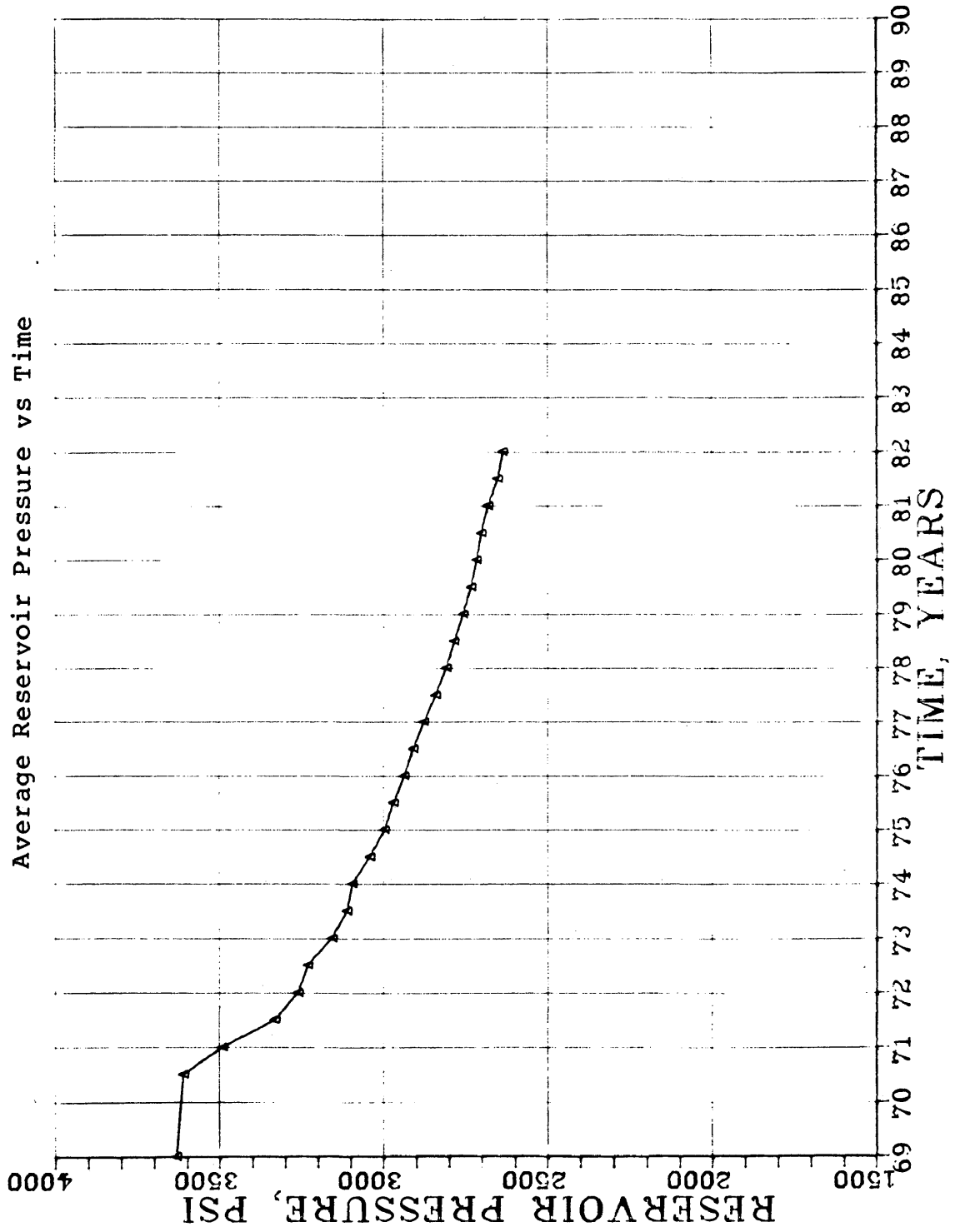


Figure 29



confirm the volumetric original oil in place. This method uses a plot of expansion per unit pressure drop, versus withdrawals per unit pressure drop (Bass, 1982).

The material balance equation is written in both sides with a pressure difference, and arranged algebraically to obtain a linear equation. The original oil-in-place is the slope of the straight line; it has also been shown that from the intercept, the aquifer radius to the reservoir radius ratio could be calculated.

Some water influx was known to exist, particularly along the southwest flank; however, it was not believed to be the dominant producing mechanism of TP13-A Sand reservoir.

When a small aquifer is connected to an oil reservoir, the aquifer can be treated not only as a finite system, but as a large storage tank. The MBE as an equation of a straight line for saturated reservoirs with water drive, original gas-cap, and without water or gas injection can then be written as:

$$Y = a + b \cdot X$$

where:

$$Y = \frac{NP_j B_{tj} + (R_{pj} - R_{si}) B_{gj} - NP_k B_{tk} + (R_{pk} - R_{si}) B_{gk} + W_{pj} B_{wj} - W_{pk} B_{wk}}{P_k - P_j}$$

$$a = \left(\frac{N B_{ti}}{1 - S_{wi}} \right) (C_w S_{wi} + C_f) + (r_a^2 / r_o^2 - 1) (C_w + C_f)$$

b=N

$$X = \frac{B_{tj} - B_{tk} + (mB_{ti}/B_{gi})(B_{gj} - B_{gk})}{P_k - P_j}$$

The derivation of this equation is presented in Appendix A.

This approach permits the generation of $(n-1)+(n-2)..+1$ data points having n pressure data, while with the conventional MBE it is possible to obtain only $(n-1)$ data points.

A computer program written to perform the calculations using the above equation is presented in Appendix B.

Three hundred values for X and Y were generated from 25 pressure points, which are plotted in Figure 30. Figure 31 is a plot of 24 X, Y values calculated with the conventional MBE using values of 0.01, 0.02, and 0.03 for the ratio of the initial gas-cap volume to the initial oil volume, m .

In these plots, the original oil-in-place is the slope of the line, and it was found to be 10.0 million STB.

The intercept of the line with the Y axis was found to be 4,598. From this value and using water compressibility, C_w , equal to 2.8×10^{-6} 1/psi (Dobson and Standing, 1944), and formation rock compressibility, C_f , equal to 14.1×10^{-6} 1/psi (Newman, 1973), the aquifer radius to the reservoir radius ratio was found to be equal 3.5. This value confirms the assumption of a small aquifer associated with the TP13-A Sand reservoir.

Figure 30
Calculation of Original Oil-In-Place TP13-A Sand

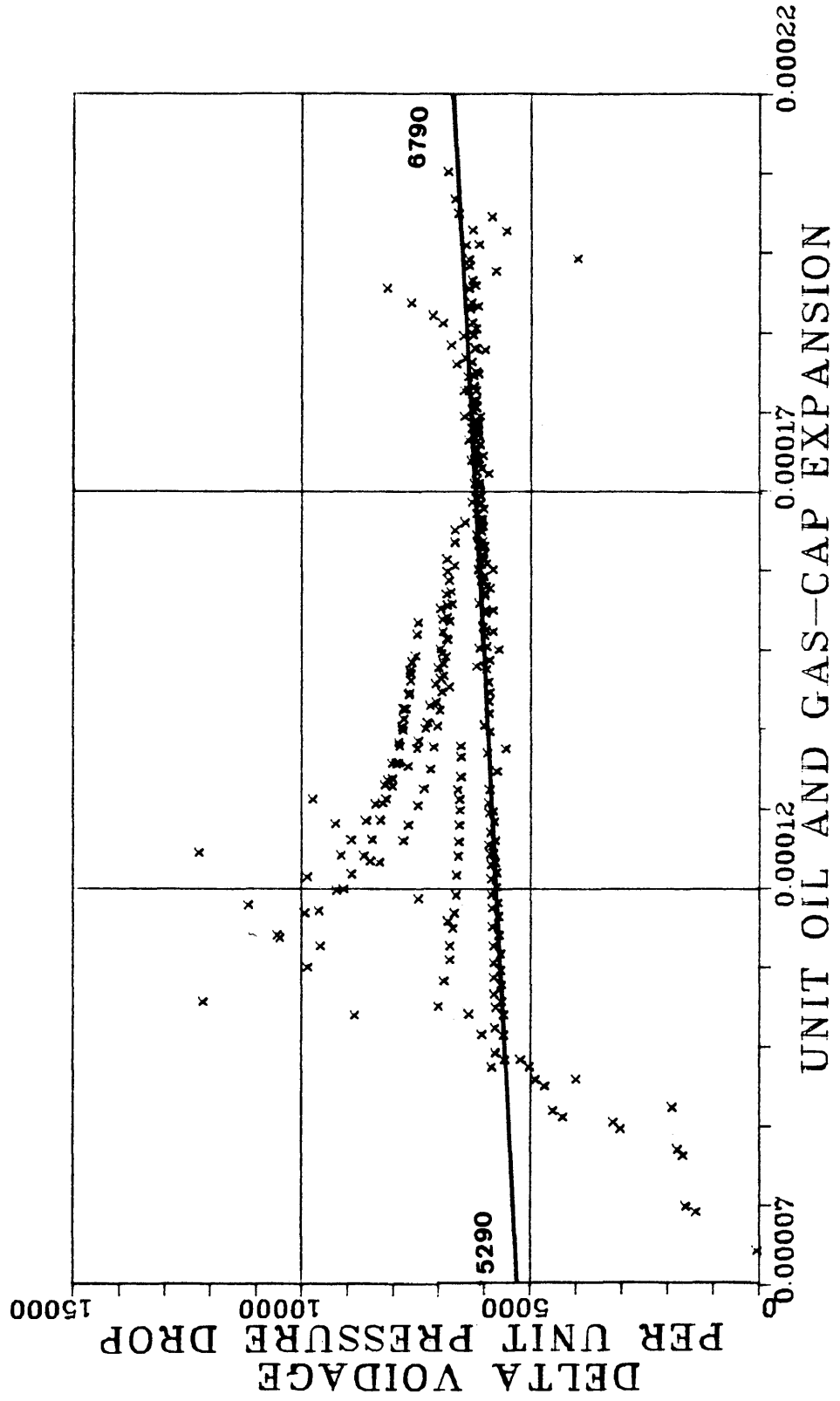
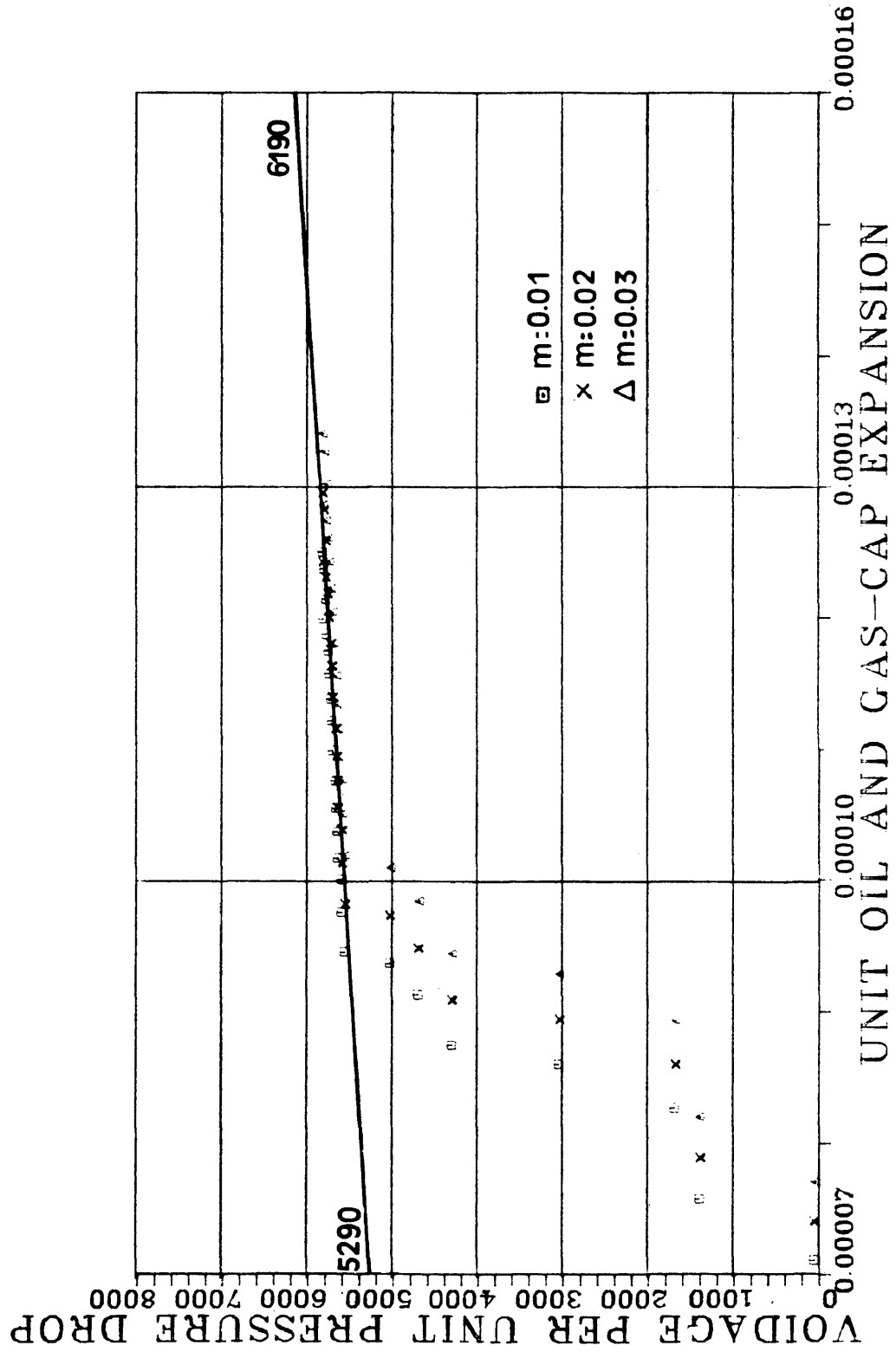


Figure 31
 Calculation Of Original Oil-In-Place TP13-A Sand
 For Different Values Of m



The difference between the volumetric (10.3 MMSTB) and the material balance (10.0 MMSTB) determinations of original oil-in-place, represents a deviation of only 3 percent; this is considered an excellent agreement.

FUTURE PERFORMANCE CALCULATIONS

Having determined the slope, b , and the intercept, a , from the material balance equation into a $Y=a+bX$ format, the future performance of TP13-A Sand reservoir was estimated by extrapolation of this straight line. The X,Y plot (Figures 30 and 31) is one of the few plots that can be extrapolated to predict the future (Bass, 1982). This approach does not imply a trial and error solution.

A computer program written to perform the calculations is presented in Appendix C. The following steps summarize the calculation procedure:

- (a) A pressure value was assumed by extrapolation of past performance data (Figure 29), and a value of X was calculated from the equation:

$$X=[B_t-B_{ti}+(mB_{ti}/B_{gi})(B_g-B_{gi})](P_i-P_n)$$

- (b) Using this value, Y was estimated from the equation:

$$Y = a + b \cdot X$$

where:

$$a = 4,598$$

$$b = N = 10.3 \text{ MMSTB}$$

- (c) Since Y is function of cumulative production and pressure, Y was solved for cumulative production:

$$NP_n = \frac{Y(P_i - P_n) - W_p}{B_t + (R_p - R_{si})B_g}$$

For future predictions, water production was assumed negligible.

(d) The cumulative gas production at the end of the prediction period was calculated from the equation:

$$GP_n = GP_{n-1} + (NP_n - NP_{n-1}) (R_{pn} - R_{pn-1}) / 2$$

where:

$$R_{pn} = \left(R_s + \frac{K_g \mu_o B_o}{K_o \mu_g B_g} \right) n$$

The first calculation requires that $R_{pn} = R_{pn-1}$ in order to calculate the oil saturation in the producing portion of the reservoir.

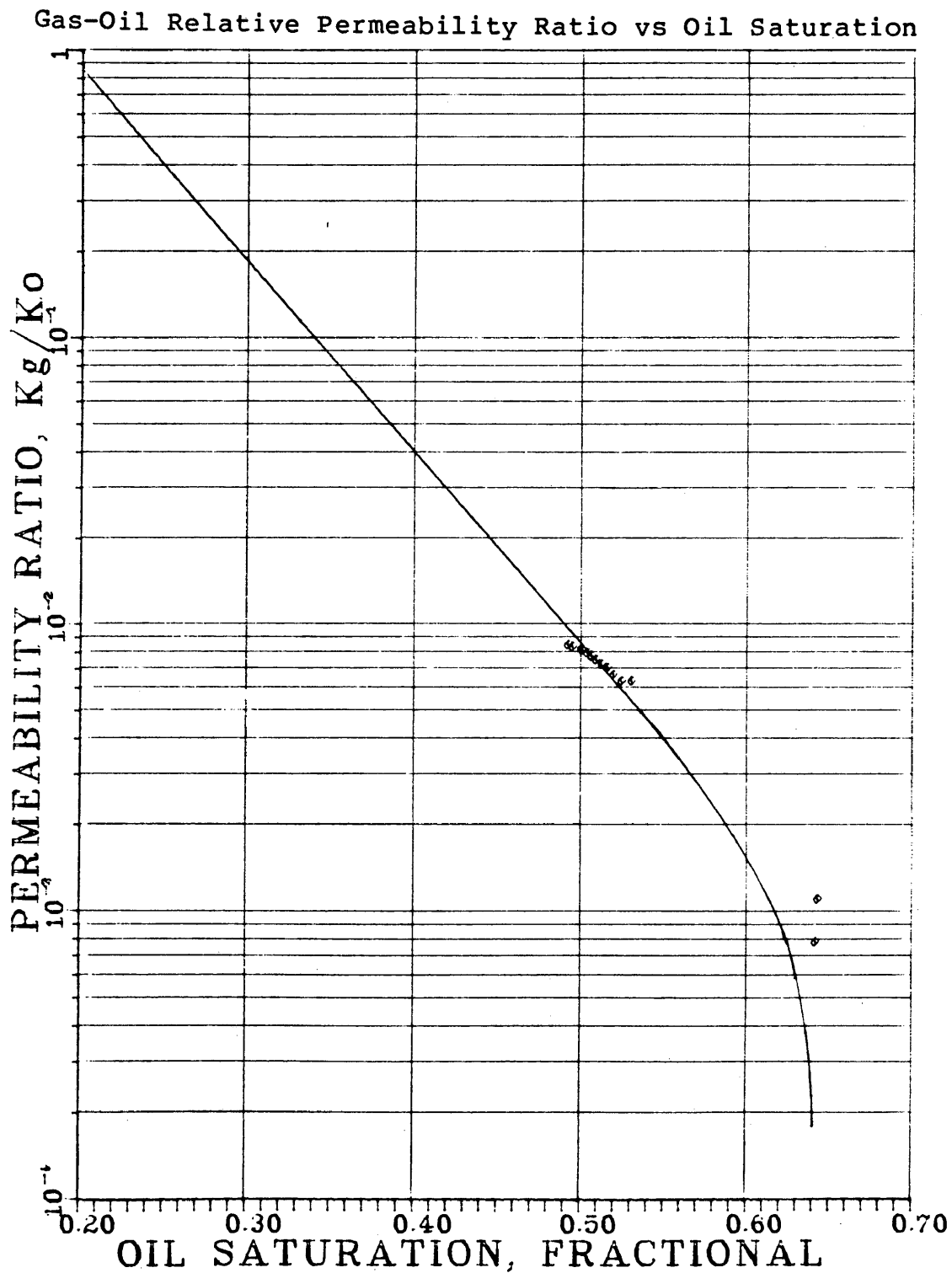
To calculate the instantaneous gas-oil ratio, R_p , a plot of K_g/K_o vs S_o is required. This plot is presented in Figure 32, and was determined from production and PVT data (Smith, 1966).

The oil saturation in the uninvaded zone was calculated from the following equation (Slider, 1976):

$$S_{oun} = \frac{(N - NP) B_o - (S_o B_Y (W_e - W_p) / (1 - S_o B_Y - S_{wi}))}{(N B_{oi} / (1 - S_{wi})) - ((W_e - W_p) / (1 - S_o B_Y - S_{wi}))}$$

This equation neglects the gas-cap expansion, and it does not account for the solution gas migration to the

Figure 32



gas-cap. As a result, the predicted GOR performance of TP13-A Sand reservoir will be somewhat higher than it would be if these factors were taken into account. In a more refined study the gas-cap expansion and the solution gas migration to the gas-cap must be considered.

The above equation also assumes that all production takes place from the uninvaded zone, and that the fractional pore volume of oil bypassed, S_{oBY} , is a constant. Since laboratory data was not available, S_{oBY} , was determined by using the reported oil saturation from conventional core analysis. A value of 18.0 percent was used in the calculations.

- (e) The cumulative water influx for the assumed pressure was calculated with the following equation, which assumes the aquifer is behaving like a large storage tank:

$$W_{en} = \pi * h * f * \phi * C_e (r_a^2 - r_o^2) (P_i - P_n) / 5.61$$

The oil reservoir radius was calculated by assuming that the total reservoir area was in the shape of a quarter circle. Since an aquifer radius to reservoir radius ratio of 3.5 was found, the aquifer radius, r_a , was determined to be 17,832 feet, from a reservoir radius, r_o , of 5,095 feet.

- (f) The volume of the reservoir that has been invaded by water, PV_{in} , was estimated as follows:

$$PVI_n = 5.61 (W_e - W_p) / (1 - S_{oBy} - S_{wi})$$

(g) The location of the oil water contact assuming an even water encroachment, was found from the above equation, and from Figure 33, which is a plot of cumulative pore-volume versus depth.

Steps (a) to (g) were repeated down to a reservoir pressure of 1,000 psi.

Since relative oil permeability measurements on cores, initial producing capacity, and capacity distribution with pore-volume were not available for TP13-A Sand, future production rates were estimated from decline curve analysis. Figure 34 is a decline curve plotted for the last several years in the producing life of the field.

Assuming an economic limit for oil production of 60 BOPD, the cumulative production at the end of each year was calculated. Table 9 lists the results of the decline curve analysis for TP13-A Sand.

Once the cumulative oil production at the end of each year was obtained, the corresponding pressure was determined from Figure 35 which is a plot of predicted pressure versus cumulative oil production.

Table 10 provides the summary of the prediction calculations. Figures 35 and 36 show the predicted pressure-production and pressure-time for TP13-A Sand reservoir.

Figure 33

Pore-Volume Distribution and Well Completion Location in The Pore-Volume

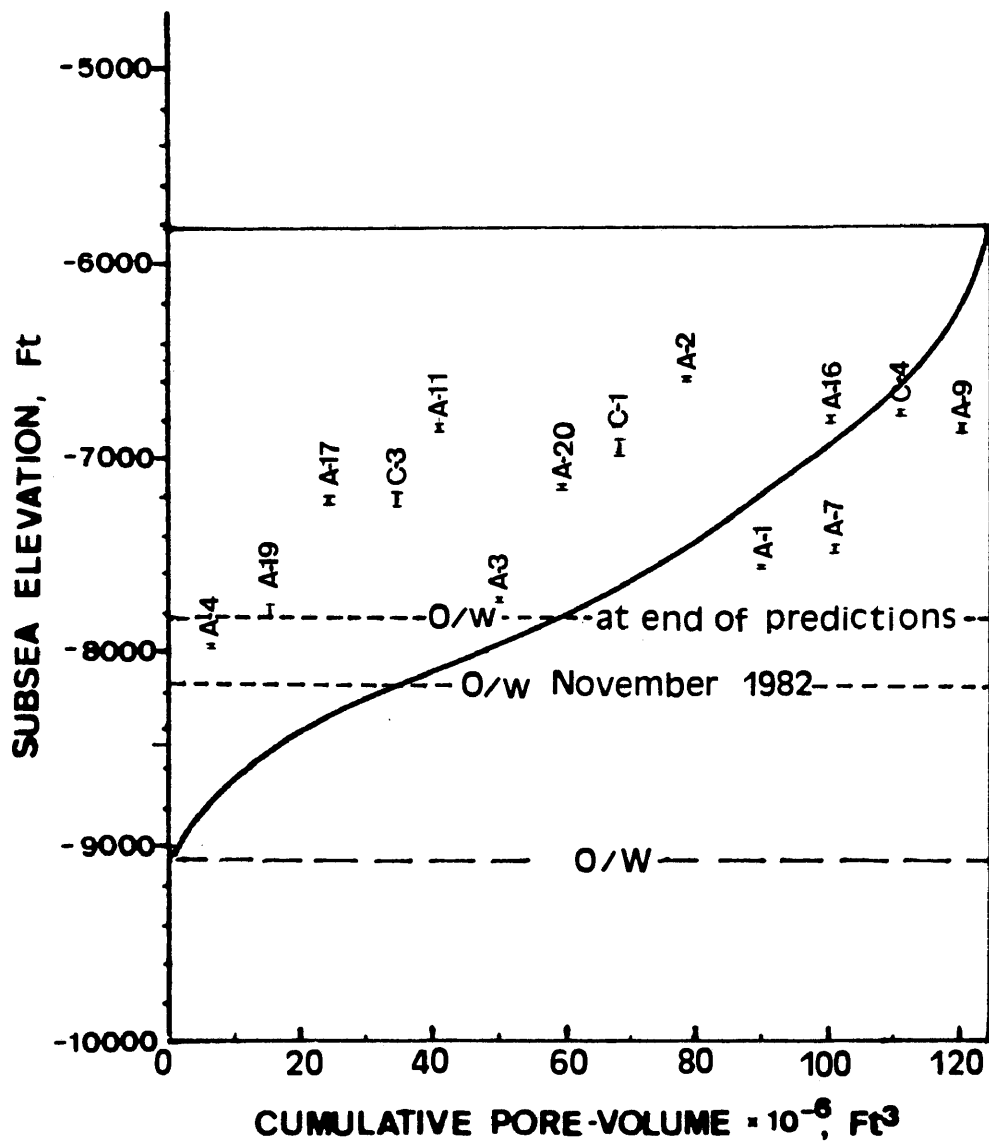


TABLE 9
Results Of Decline Curve Analysis TP13-A Sand

Year End	Oil Rate BOPD	Oil Production STB	Cumulative STB
1983	957	410,358	3,810,358
1984	699	299,774	4,110,132
1985	511	218,990	4,329,122
1986	373	159,977	4,489,099
1987	273	116,866	4,605,965
1988	199	85,373	4,691,338
1989	145	62,367	4,753,705
1990	106	45,560	4,799,265
1991	78	33,284	4,832,549
1992	57	24,313	4,856,862

Figure 35

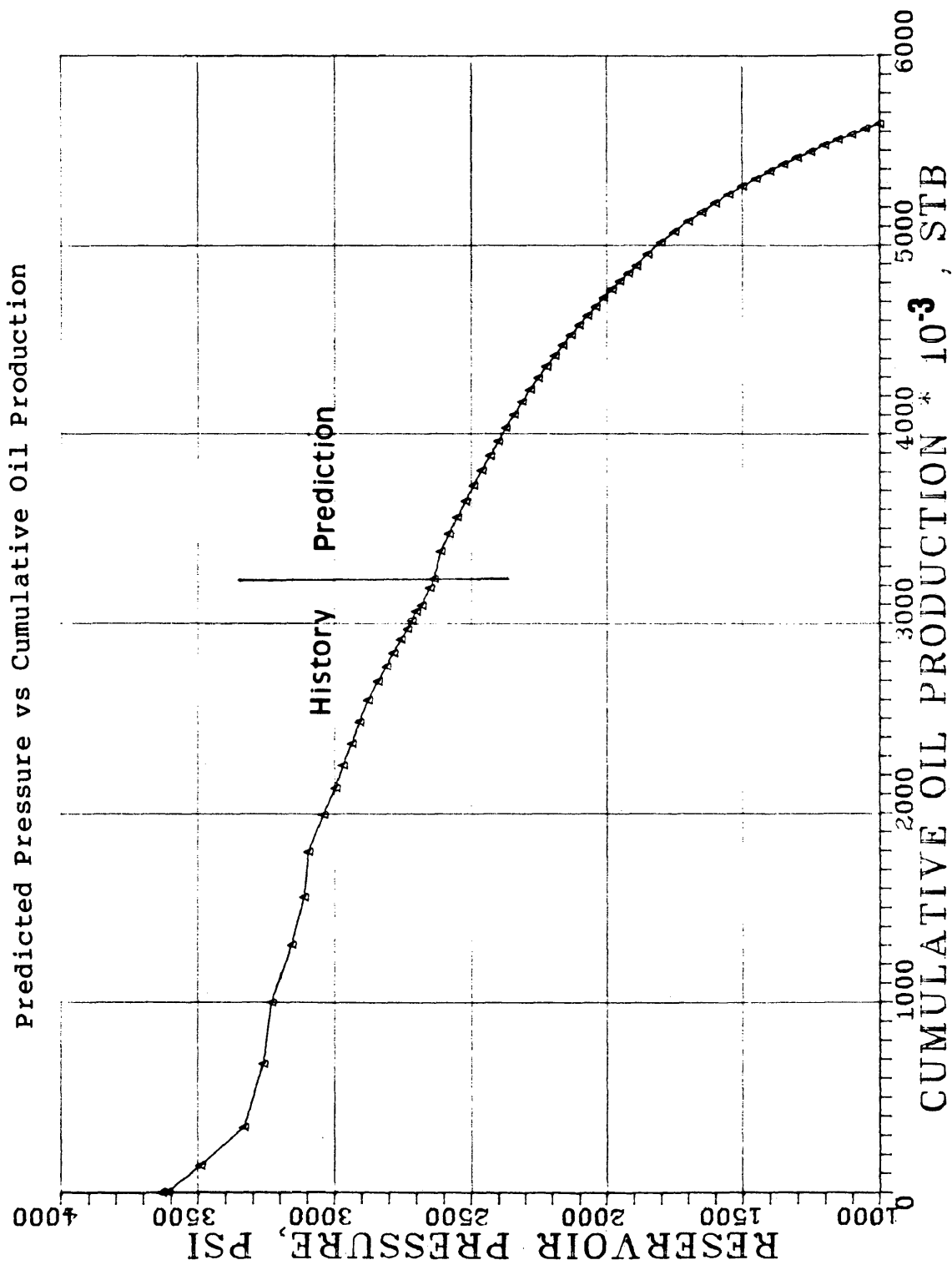
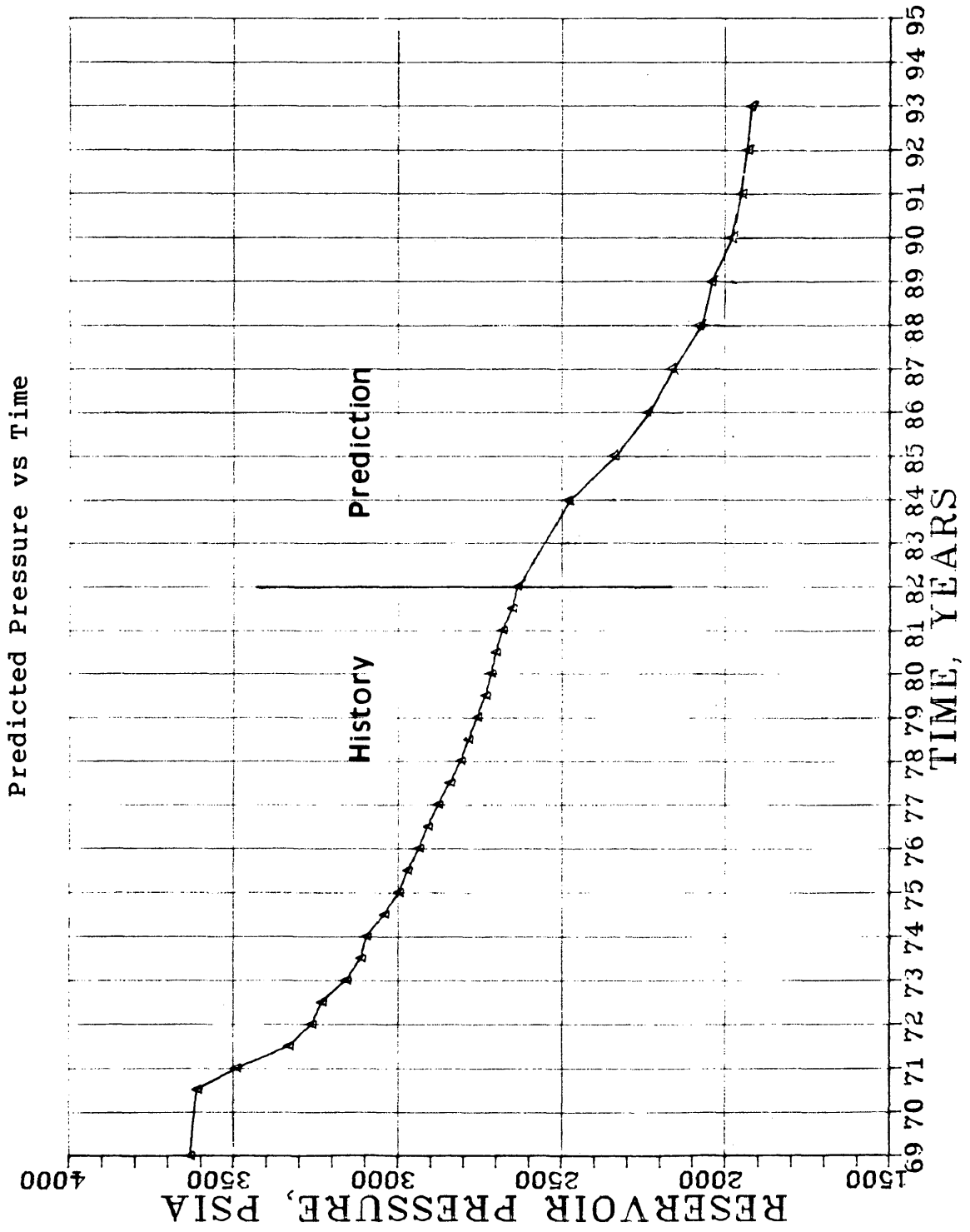


TABLE 10
Summary Of Future Predictions-TP13-A Sand

Year End	Cumulative Oil Production (MMBbls)	Cumulative Gas Production (BSCF)	Cumulative Water Influx (MMBbls)	Pore- Volume Invaded MM cu.ft	Pressure (psia)
1983	3.81	3.60	3.29	39.4	2,470
1984	4.11	4.10	3.72	44.7	2,330
1985	4.33	4.48	4.01	48.2	2,230
1986	4.49	4.70	4.22	50.8	2,155
1987	4.61	5.00	4.47	53.7	2,070
1988	4.69	5.18	4.55	54.8	2,040
1989	4.75	5.36	4.72	56.9	1,980
1990	4.80	5.42	4.79	57.8	1,955
1991	4.83	5.51	4.87	58.6	1,930
1992	4.86	5.57	4.89	59.0	1,920

Figure 36



The ultimate primary recovery was estimated to be 4.86 million STB of oil, or 47 percent of the original oil-in-place. Reservoir pressure will decline to 1,920 psi, and the producing gas-oil ratio will raise to 2,406 SCF/STB.

The cumulative water influx calculated amounted to 4.89 million barrels, and the pore-volume invaded at abandonment pressure of 1,920 psi amounted to 59 million cu.ft.

Figures 37 and 38 are plots of producing GOR, and water influx versus cumulative oil production, respectively.

Figure 37

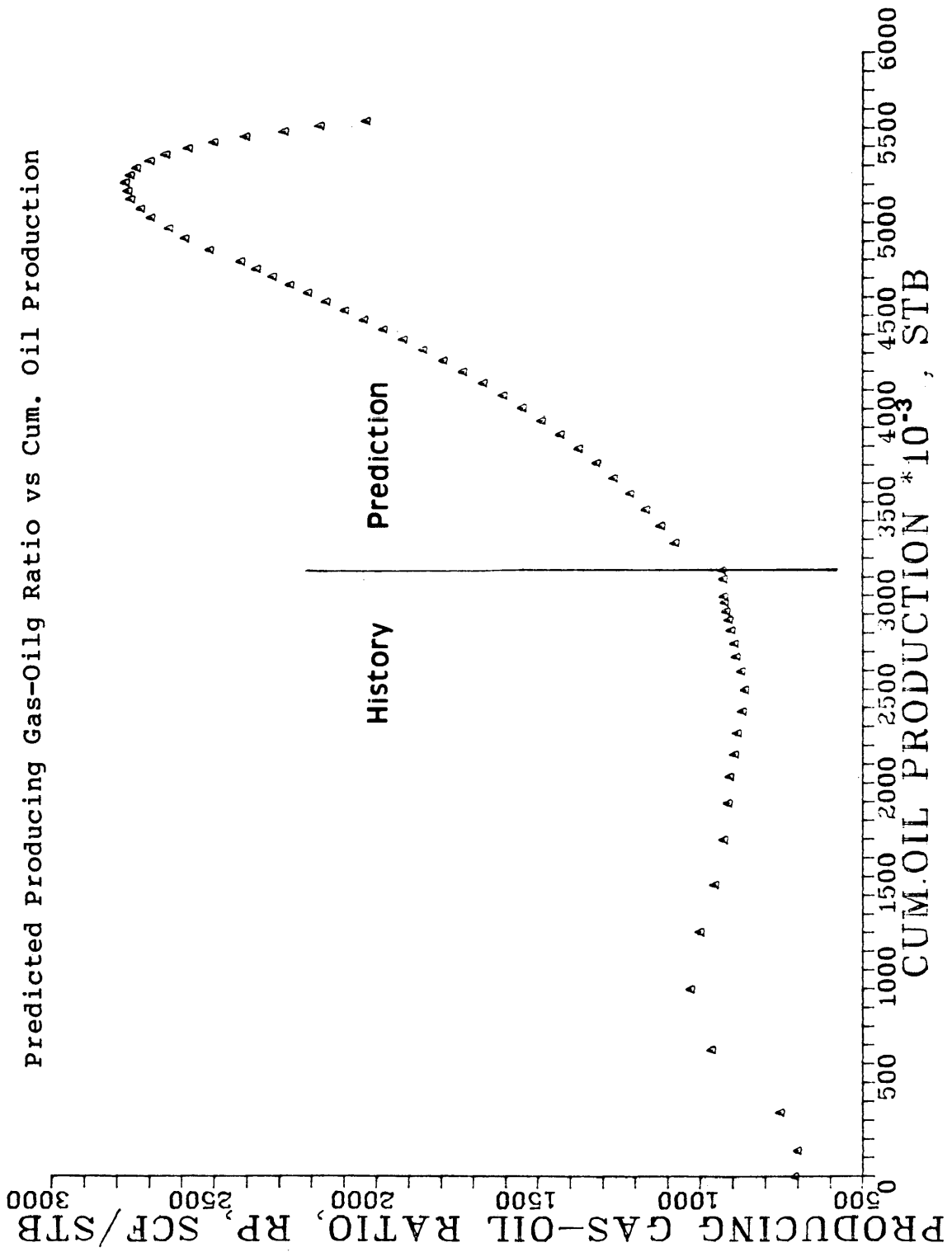
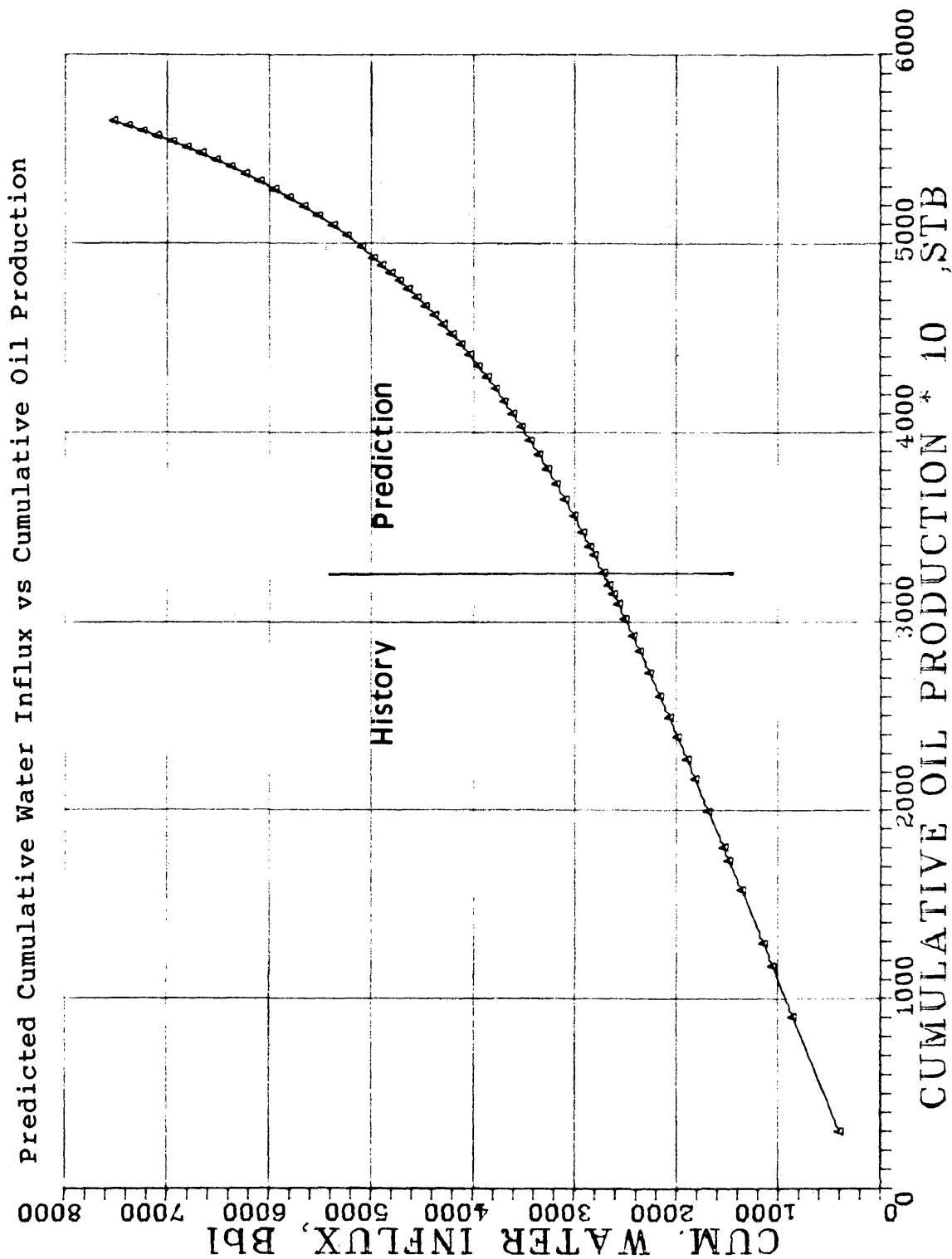


Figure 38



CONCLUSIONS

From the results of the reservoir study, of TP13-A Sand reservoir, the following conclusions can be made:

1. The original oil-in-place based on pore-volume calculations, and based on material balance equation is estimated to be 10.3 million STB.
2. The size of the gas-cap is minor in relation to that of the oil reservoir. The initial free gas-in-place is estimated to be 356 MMSCF.
3. The aquifer radius to the reservoir radius ratio is estimated to be 3.5.
4. The oil recovery to November, 1982, has been about 33 percent of stock-tank oil originally in place.
5. Some water was produced from downdip wells located in the southeast portion of the field (wells A-1, A-3, and A-7). Probably mechanical problems rather than water encroachment is the source of the water produced.
6. Water influx was quite limited, and its effects were not sufficient to maintain pressure throughout the entire reservoir; however, at abandonment pressure of 1,920 psia, the net water influx will replace approximately 48 percent of the pore volume, having

noticeable effect on the over-all pressure-production performance of TP13-A Sand reservoir.

7. In absence of a strong water drive, and due to the great structural relief of TP13-A Sand reservoir, it is believed that the drive mechanism is primarily solution-gas with gravity segregation.
8. Oil and gas segregation has been effective in maintaining a high oil saturation in down flank wells. This is evidenced by the GOR performance of the individual wells, as noted from declines in GOR of down structure wells.
9. The pronounced dip and the favorable sand and fluid characteristics, make gravity segregation particularly effective.
10. The study indicates that the ultimate oil recovery by primary depletion methods will amount 4.86 million STB or 47 percent of the original oil-in-place, and that the remaining life of the reservoir will be 10 years.

REFERENCES CITED

- Amyx, J.W., Bass, D.M., and Whilting, R.L., 1960, Petroleum Reservoir Engineering: New York, McGraw Hill Book Co.
- Bankhead, C.Jr., McCord, D.R., and Associates, Inc., 1970, "Processing of Geological and Engineering Data in Multipay Fields for Evaluation", Dallas, Texas, Society Of Petroleum Engineers of AIME, SPE Reprint Series No.3, pp. 8-23.
- Bass, D.M., 1982, PE-607 Class notes.
- Beggs, H.D., and Robinson, J.F., 1975, "Estimating the Viscosity of Crude Oil Systems", JPT, Sep., pp. 1140-1141.
- Davis, D.G., 1982, PE-519 Class notes.
- Dodson, C.R., and Standing, M. B., 1944, "Pressure Volume Temperature and Solubility Relation for Natural Gas-Water Mixtures", Dallas, Texas, Drilling and Production Practice, American Petroleum Institute.
- Franklin, L.O., Koederitz, W.A., and Walker, D., 1975, "Recovering Attic Oil", Dallas, Texas, Society Of Petroleum Engineers of AIME, SPE Reprint Series No.4a pp. 99-104.
- Frick, J.C., 1962, Petroleum Production Handbook, Dallas, Texas, SPE of AIME, v. 2, p. 24-8.

- Halbouty, M.T., 1979, Salt Domes Gulf Region, United States and Mexico, Houston, Texas, Gulf Publishing Co., pp. 90-101.
- Hall, K. R. and Yarborough, L., 1974, "How to Solve Equation of State for Z-Factors", The Oil and Gas Journal, Feb. 18th, pp. 86-88.
- Newman, G. H., 1973, "Pore Volume Compressibility of Consolidated, Friable, and Unconsolidated Reservoir Rocks Under Hydrostatic Loading", JPT, v. 25, pp. 129-134.
- Slider, H. C., 1976, Practical Petroleum Reservoir Engineering Methods, Tulsa, Oklahoma, Petroleum Publishing Co., p. 357.
- Smith, C. R., 1966, Mechanics of Secondary Oil Recovery, New York, Reinhold, p. 45.
- Van Everdingen, A. F., and Hurst, W., 1949, "The Application of The Laplace Transformation to Flow Problems in Reservoirs", Am. Inst. Mining Metall. Petroleum Engineers Trans., v. 186, pp. 305-324.
- Vasquez A., M. E., and Beggs, H. D., 1980, "Correlations for Fluid Physical Property Prediction", JPT, Jun., pp. 968-970.

NOMENCLATURE

- Bt = total oil formation volume factor, bbl/STB
- GP = cumulative gas produced, SCF
- Kg = effective permeability to gas, mD
- Ko = effective permeability to oil, mD
- m = ratio of initial gas-cap-reservoir volume to initial reservoir oil volume
- N = Initial oil-in-place, STB
- NP = cumulative oil produced, STB
- Pi = initial reservoir pressure, psia
- Pn = reservoir pressure at time n, psia
- RPn = producing gas-oil-ratio at time n, SCF/STB
- Rs = solution gas-oil-ratio, SCF/STB
- Rsi = initial solution gas-oil-ratio, SCF/STB
- Soun = average oil saturation in the uninvaded zone, fraction of pore volume
- SoBY = average oil saturation in the invaded zone, fraction of pore volume
- Swi = initial water saturation, fraction of pore volume
- We = cumulative water influx, Bbl
- Wp = cumulative water production, Bbl
- μ_g = gas viscosity, cP
- μ_o = oil viscosity, cP
- n = time interval

APPENDIX A

DERIVATION OF THE MATERIAL BALANCE EQUATION AS
AN EQUATION OF A STRAIGHT LINE (Bass, 1982)

The material balance equation for saturated reservoirs with water drive, original gas-cap and without water or gas injection, written in both sides of the equation with a pressure difference is:

$$N(B_{tj}-B_{jk})+N\frac{B_{ti}}{1-S_{wi}}(C_w S_{wi}+C_f)(P_k-P_j)+N m\frac{B_{ti}}{B_{gi}}(B_{gj}-B_{gk})+$$

$$W_{ej}-W_{ek} = NP_j B_{tj}+(RP_j-R_{si})B_{gj} -NP_k B_{tk}+(RP_k-R_{si})B_{gk} + \\ W_{pj} B_{wj} - W_{pk} B_{wk} \quad (1)$$

- where: N = initial oil-in-place, STB
 B_t = total oil formation volume factor, bbl/STB
 S_{wi} = average initial water saturation, fractional
 C_w = water compressibility, vol/vol/psi
 C_f = formation rock compressibility, vol/vol/psi
 m = ratio of initial gas-cap reservoir volume to initial reservoir oil volume
 B_g = gas formation volume factor, bbl/SCF
 W_e = cumulative water influx, Bbl
 NP = cumulative oil produced, STB
 RP = cumulative GOR, SCF/STB
 R_{si} = initial solution gas-oil ratio, SCF/STB

$$\begin{aligned}
 W_p &= \text{cumulative water production, Bbl} \\
 B_w &= \text{water formation volume factor, bbl/STB} \\
 i &= \text{initial conditions} \\
 j &= 0, n-1 \\
 k &= j+1, n \\
 n &= \text{number of pressure data} \\
 B_t &= B_{oi} + (R_{si} - R_s) B_{gi} \quad (2)
 \end{aligned}$$

For a radial system the water influx can be approximated by the use of unsteady state water influx equation:

$$W_{en} = \frac{2\pi f \phi h C_e n}{5.61} \sum_{j=1}^n [Q(t_{Dn} - t_{Dj-1}) \Delta P_j] \quad (3)$$

$$\text{where: } t_D = \frac{0.006328 k t}{\phi \mu C_e r_o^2} \quad (4)$$

t = time, days

k = permeability, md

μ = viscosity, cp

C_e = $C_w + C_f$, vol/vol/psi

r_o = reservoir radius, ft

f = encroachment angle/360

ΔP_j = $(P_0 - P_1)/2$

ΔP_j = $(P_{j-2} - P_j)/2$ for $j \geq 2$

$Q(t_D)$ = dimensionless water influx function,
(Van Everdingen and Hurst, 1949).

Series of influx calculations have shown that when a small aquifer is connected to an oil reservoir the aquifer can be treated not only as a finite system, but like a large storage tank. In this case, the $Q(tD)$ term becomes a constant, equal to:

$$\frac{1}{2} \text{ra2/ro2} - 1 \quad (5)$$

and ΔP becomes $(P_i - P_n)$ such that,

$$W_e = \frac{\pi * h * f * \phi * C_e (\text{ra2} - \text{ro2}) (P_i - P_n)}{5.61} \quad (6)$$

If N is defined as:

$$N = \frac{\phi * \pi * \text{ro2} * h (1 - S_{wi})}{B_{ti}} \quad (7)$$

$$W_{en} = \left(\frac{N * B_{ti}}{1 - S_{wi}} \right) (C_w + C_f) (\text{ra2/ro2} - 1) (P_i - P_n) \quad (8)$$

The material balance equation can then be written as,

$$N (B_{tj} - B_{tk}) + m \frac{B_{ti}}{B_{gi}} (B_{gj} - B_{gk}) + \frac{N B_{ti}}{(1 - S_{wi})} (C_w S_{wi} - C_f) +$$

$$(\text{ra2/ro2} - 1) (C_w + C_f) (P_j - P_k) = N P_j B_{tj} + (R P_j - R_{si}) B_{gi} -$$

$$N P_k B_{tk} + (R P_k - R_{si}) B_{gk} + W_{pj} B_{wj} - W_{pk} B_{wk} \quad (9)$$

This equation is arranged algebraically, resulting in a linear equation as follows:

$$Y = a + b \cdot X \quad (10)$$

were:

$$Y = \frac{\Delta \text{VOIDAGE}}{(P_k - P_j)}$$

$$a = \left(\frac{N \cdot B_{ti}}{1 - S_{wi}} \right) (C_w S_{wi} + C_f) + (r_{a2}/r_{o2} - 1) (C_w + C_f)$$

$$b = N$$

$$X = \frac{B_{tj} - B_{tk} + (m B_{ti}/B_{gi}) (B_{gj} - B_{gk})}{(P_k - P_j)}$$

APPENDIX B

PROGRAM TO CALCULATE THE X, Y VALUES FROM THE MATERIAL
BALANCE EQUATION AS AN EQUATION OF A STRAIGHT LINE, FOR
A SATURATED OIL RESERVOIR.

```

      DIMENSION P(0:40), GP(0:40), WP(0:40), BG(0:40), RS(0:30), BO(0:30),
      1BT(30), RP(30), X1(0:30,30), Y1(0:30,30)
      REAL NP(0:40), M(3)
      M(2)=0.02
      READ(1,1)(P(I),NP(I),GP(I),WP(I),I=0,24)
      1  FORMAT(4G)
      *****
      DISOLVED GOR CONSTANTS
      *****
      DATA C1,C2,C3/0.0178,1.1870,23.931/
      OIL FVF CONSTANTS
      *****
      DATA CB1,CB2,CB3/4.67E-4,1.1E-5,1.337E-9/
      PSEUDO CRITICAL PRESSURE AND TEMPERATURE DATA
      *****
      DATA CO,XN1,DS,IFLG/0.20,0.22,0.7,0/
      Z-FACTOR DATA
      *****
      DATA T,NZ/614.0,2/
      RESERVOIR DATA
      *****
      DATA SPG,API,TS,PS,SWI,CW,CF/0.6014,35.,60.,50.,0.36,2.8E-6,
      114.1E-6/
      CONSTANT VALUES TO COMPUTE DISSOLVED GOR
      *****
      SPGC=SPG*(1.+5.912E-5*API*TS*ALOG10(PS/114.7))
      A1=C3*API/T
      CALCULATE P V T DATA
      *****
      .....Calculate pseudo critical P and T
      CALL CRITP(SPG,CO,XN,DS,IFLG,PCF,TCR)
      DO 10 I=0,24
      PP=P(I)
      CALL ZFACT(Z1,PP,T,PCR,TCR,NZ,IFL)
      .....Calculate Gas FVF [bbl/STB]
      BG(I)=0.00515*T*Z1/P(I)
      .....Calculate Dissolved GOR [SCF/STB]
      RS(I)=C1*SPGC*P(I)**C2*EXP(A1)
      .....Calculate Oil FVF [bbl/STB]
      BO(I)=1.+CB1*RS(I)+(T-520.)*(API/SPGC)*(CB2+CB3*RS(I))
      BT(I)=BO(I)+(RS(I)-RS(0))*BG(I)
      IF(I.EQ.0) GO TO 15
      RP(I)=GP(I)*1000.0/NP(I)
      15 CONTINUE
      10 CONTINUE
      BT(0)=BO(0)
      RP(0)=0.0

```

CALCULATE UNIT OIL EXPANSION (Y1) AND DELTA(VOIDAGE)/(Pk-Pj) (X1)

```

DO 20 J=0,23
DO 30 K=J+1,24
CC=M(2)*(BO(0)/BG(0))*(BG(J)-BG(K))
X1(J,K)=(BT(J)-BT(K)+CC)/(P(K)-P(J))
AA=NP(J)*(BT(J)+(RP(J)-RS(0))*BG(J))
BB=NP(K)*(BT(K)+(RP(K)-RS(0))*BG(K))
Y1(J,K)=((AA-BB)+WP(J)-WP(K))/(P(K)-P(J))
30 CONTINUE
20 CONTINUE

```

WRITE DATA IN FILES FOR LATER TABULATING AND PLOTTING

```

DO 50 J=0,23
DO 60 K=J+1,24
WRITE(8,3)X1(J,K),Y1(J,K)
50 CONTINUE
3 FORMAT (2G)
STOP
END

```

APPENDIX C

PROGRAM TO PREDICT THE FUTURE BEHAVIOR OF A SATURATED OIL RESERVOIR, USING THE MATERIAL BALANCE AS AN EQUATION OF A STRAIGHT LINE.

```

DIMENSION P(0:50),GP(0:50),BG(0:50),RS(0:50),BO(0:50),
IBI(0:50),RP(0:50),UC(0:50),UG(0:50),PVI(50),WF(50),S0(50),
IRCN(50),RC(0:50),DNP(50)
REAL NP(0:50),M,KGKO

*****
PSEUDO CRITICAL PRESSURE AND TEMPERATURE DATA
*****
DATA CO,XN1,DS,IFLG/0.30,0.22,7.0,0/

Z-FACTOR DATA
*****
DATA T,NZ/614.0,2/

RESERVOIR FLUIDS AND ROCK DATA
*****
DATA SPG,API,TS,PS,SWI,SOR,N,M/2.6014,35.,60.,50.,7.36,3.18,
110.3E6,0.02/
DATA CW,CF,AINT,RA,RC,H,PUR/2.8E-6,14.1E-6,4598.,17832.,5095.,
123.0,0.27/

READ VALUES FOR ASSUMED PRESSURE
*****
JP=43
READ(2,3)(P(I),I=0,JP)
3 FORMAT(1G)
NOTE: P(0) equal to the initial reservoir pressure.

*****
INITIAL PRODUCTION DATA FOR PREDICTION
*****
NP(0)=3231999.
GP(0)=3024009.E3
WP=57800.
RC(0)=GP(0)/NP(0)
RP(0)=RC(0)

*****
CALCULATE GAS FVF, bbl/SCF, AND GAS VISCOSITY, CR.
*****
.....Calculate pseudo critical P and T
CALL CRITP(SPG,CO,XN,DS,IFLG,PCR,TCR)
DO 10 I=0,JP
PP=P(I)
CALL ZFACT(Z1,PP,T,PCR,TCR,NZ,IFL)
.....Calculate Gas FVF [bbl/STB]
BG(I)=0.00515*T*Z1/P(I)
CALL VISC(VIS,PP,Z1,T,SPG)
UG(I)=VIS
10 CONTINUE

*****
CALCULATE PVT CORRELATION DATA
*****
CALL OILPRO(RS,BO,BT,UC,P,BG,T,API,SPG,TS,PS,JP)
111 WRITE(10,111)(P(I),BO(I),UD(I),UG(I),RS(I),BG(I),I=0,JP)
FORMAT(1X,F7.1,3X,F6.4,3X,F8.5,3X,F8.5,3X,F6.2,3X,F10.6)

PREDICTION OF THE FUTURE BEHAVIOR
*****

```

```

BWF=3.14159*(1./6.)*H*PJR*(CW+CF)*(RA*RA-RO*RO)/5.61
DO 20 I=1,JP
Y=AINT+N*(BT(I)-BT(0))+M*(BT(0)/BG(0))*(BG(I)-BG(0))/(P(0)-
1P(I))
50 WE(I)=BWE*(P(0)-P(I))
NP(I)=(Y*(P(0)-P(I))-WP)/(BT(I)+(RC(I-1)-RS(0))*BG(I))
RESOIL=(N-NP(I))*BO(I)-SOR*(WE(I)-WP)/(1.-SOR-SWI)
RESPV=(N*BO(0)/(1.-SWI))-((WE(I)-WP)/(1.-SOR-SWI))
SO(I)=RESOIL/RESPV
X1=1.2625649-6.6597949*SQ(I)
KGKO=10.**X1
RP(I)=RS(I)+KGKO*(UQ(I)/UG(I))*(BO(I)/BG(I))
PVI(I)=5.61*(WE(I)-WP)/(1.-SOR-SWI)
33 WRITE(4,33)Y,KGKO
FORMAT(2G)
GP(I)=GP(I-1)+((RP(I-1)+RP(I))/2.)*(NP(I)-NP(I-1))
RCN(I)=GP(I)/NP(I)
DELT=ABS(RCN(I)-RC(I-1))
IF(DELT.LE.20.) GO TO 40
RC(I-1)=RCN(I)
40 GO TO 50
RC(I)=RCN(I)
DNP(I)=NP(I)-NP(I-1)
20 CONTINUE
55 WRITE(6,55)
FORMAT(1X,6X,'P',13X,'NP',12X,'DNP',14X,'GP',11X,
1'RP',15X,'RC',12X,'WE',13X,'PV'(/)
WRITE(6,1)(P(I),NP(I),DNP(I),GP(I),RP(I),RC(I),WE(I),
1PVI(I),I=1,JP)
1 FORMAT(8G)
STOP
END

```

```

***** SUBROUTINE OILPRO(RS,BO,BT,UQ,P,BG,T,API,SPG,TS,PS,JP)
*****
* SUBROUTINE TO GENERATE PVT CORRELATION DATA USING THE *
* EQUATIONS DEVELOPED BY VASQUEZ A., AND BEGGS H. D. *
* REF: 1)"Correlations For Fluid Physical Property *
* Prediction", JPT (June, 1984) pp. 968-972 *
* 2)"Estimating The Viscosity of Crude Oil Systems", *
* JPT (Sept., 1975) pp. 1140-1141 *
*****

```

INPUT VARIABLES

```

P=PRESSURE,psia
RG=GAS FVF,bbl/SCF
T=TEMPERATURE,R
API=OIL GRAVITY,API
SPG=GAS GRAVITY(air=1)
PS=ACTUAL SEPARATOR PRESSURE,psia
TS=ACTUAL SEPARATOR TEMPERATURE,R
JP=NUMBER OF PRESSURE DATA

```

OUTPUT VARIABLES

```

RS=DISSOLVED GOR,scf/STB
BO=OIL FVF,bbl/STB
BT=TOTAL OIL FVF,bbl/STB
UQ=OIL VISCOSITY,cp.

```

LIMITATIONS

- 1) VALID FOR SATURATED OIL $P < P_b$
- 2) VALID FOR OIL GRAVITY VALUES > 30 API

```

DIMENSION RS(J:50),BC(0:50),BT(0:50),UO(0:50),P(0:50),BG(J:50)
DATA C1,C2,C3/0.0178,1.1870,23.931/
DATA CB1,CB2,CB3/4.67E-4,1.17E-5,1.337E-9/
DO 30 I=0,JP
SPGC=SPGC*(1.+5.912E-5*API*TS*ALOG10(PS/114.7))
A1=C3*API/T
RS(I)=C1*SPGC*P(I)**C2*EXP(A1)
BO(I)=1.+CB1*RS(I)+(T-520.)*(API/SPGC)*(CB2+CB3*RS(I))
IF(I.EQ.0)GO TO 10
BT(I)=BO(I)+(RS(0)-RS(I))*BG(I)
GO TO 20
10 BT(0)=BO(0)
20 T1=T-460.
Z=3.0324-0.02023*API
Y=10.**Z
X=Y/(T1**1.163)
UOD=10.**X-1.
A=10.715/((RS(I)+100.))**0.515)
B=5.44/((RS(I)+150.))**2.338)
UO(I)=A*UOD*B
30 CONTINUE
RETURN
END

```